Title
A Calcineurin-dependent Switch Controls the Trafficking Function of alpha-Arrestin Aly1/Art6

Journal
JOURNAL OF BIOLOGICAL CHEMISTRY, 288(33)

Authors
O'Donnell, Allyson F
Huang, Laiqiang
Thorner, Jeremy
et al.

Publication Date
2013

DOI
10.1074/jbc.M113.478511

Peer reviewed

THE JOURNAL OF BIOLOGICAL CHEMISTRY VOL. 288, NO. 33, pp. 24063–24080, August 16, 2013

A Calcineurin-dependent Switch Controls the Trafficking Function of α-Arrestin Aly1/Art6*[S]

Received for publication, April 17, 2013, and in revised form, June 29, 2013 Published, JBC Papers in Press, July 3, 2013, DOI 10.1074/jbc.M113.478511

Allyson F. O'Donnell[‡§¶1], **Laiqiang Huang**[‡2], **Jeremy Thorner**[§], **and Martha S. Cyert**[‡3]

From the [‡]*Department of Biology, Stanford University, Stanford, California 94305-5020, the* [§]*Department of Molecular and Cell Biology, University of California, Berkeley, California 94720-3202, and the* [¶]*Department of Cell Biology, University of Pittsburgh, Pittsburgh, Pennsylvania 15261*

Background: In response to nutrient signals, α-arrestins selectively regulate trafficking of membrane transporters.
Results: Aly1 is a substrate of the phosphatase calcineurin, and dephosphorylation triggers Aly1-dependent internalization of the permease Dip5.
Conclusion: Endocytic function of α-arrestins is stimulated by removal of inhibitory phosphorylation.
Significance: These insights define a molecular mechanism controlling the function of an α-arrestin in endocytosis, which is critical for cellular adaptation.

Proper regulation of plasma membrane protein endocytosis by external stimuli is required for cell growth and survival. In yeast, excess levels of certain nutrients induce endocytosis of the cognate permeases to prevent toxic accumulation of metabolites. The α-arrestins, a family of trafficking adaptors, stimulate ubiquitin-dependent and clathrin-mediated endocytosis by interacting with both a client permease and the ubiquitin ligase Rsp5. However, the molecular mechanisms that control α-arrestin function are not well understood. Here, we show that α-arrestin Aly1/Art6 is a phosphoprotein that specifically interacts with and is dephosphorylated by the Ca^{2+}- and calmodulin-dependent phosphoprotein phosphatase calcineurin/PP2B. Dephosphorylation of Aly1 by calcineurin at a subset of phospho-sites is required for Aly1-mediated trafficking of the aspartic acid and glutamic acid transporter Dip5 to the vacuole, but it does not alter Rsp5 binding, ubiquitinylation, or stability of Aly1. In addition, dephosphorylation of Aly1 by calcineurin does not regulate the ability of Aly1 to promote the intracellular sorting of the general amino acid permease Gap1. These results suggest that phosphorylation of Aly1 inhibits its vacuolar trafficking function and, conversely, that dephosphorylation of Aly1 by calcineurin serves as a regulatory switch to promote Aly1-mediated trafficking to the vacuole.

Cellular adaptation to environmental changes requires tight regulation of cell surface proteins. Specific ligands, excess nutrients, or stress factors induce endocytosis of plasma membrane receptors and permeases, thereby impacting nearly every aspect of cell physiology. Thus, a dynamic interplay exists between such extrinsic signals and endocytosis of specific membrane proteins, whose removal from the cell surface can alter intracellular signaling (1). One of the clearest examples of this interplay is the regulation of G-protein-coupled receptors (GPCRs)[4] by the β-arrestin class of trafficking adaptors. In mammalian cells, agonist-stimulated GPCRs initiate intracellular signaling that leads to feedback phosphorylation of the receptor (2, 3) and, in several cases, dephosphorylation of β-arrestins (4–6). Dephosphorylated β-arrestins associate with the plasma membrane and bind both GPCRs and clathrin to stimulate GPCR endocytosis (4–10). GPCR removal from the plasma membrane dampens signaling. Although β-arrestin function is clearly regulated by phosphorylation, in many cases the kinases and phosphatases responsible for this regulation have not been identified.

A related protein family, the α-arrestins (also known as arrestin-related trafficking adaptors in *Saccharomyces cerevisiae* or arrestin domain-containing proteins (ArrDCs) in mammalian cells) are conserved across eukaryotes, with 14 members in yeast and at least 6 in mammals (11–14). Hallmarks of these proteins include N-terminal arrestin-fold domains and a C-terminal tail containing dispersed copies of a sequence motif, PP*XY* (and variants thereof), which are sites for interaction with a HECT domain ubiquitin ligase (Rsp5 in yeast and Nedd4 in mammals) (15, 16). The yeast α-arrestins regulate signal-induced endocytosis (12, 17–21) and intracellular sorting of nutrient permeases (22–25). Thus, α-arrestins are adaptors

* This work was supported, in whole or in part, by National Institutes of Health Grants R01 GM-48728 (to M. S. C.), R01 GM-21841 (to J. T.), and R01 DA014204-11 (to A. Sorkin, University of Pittsburgh). This work was also supported by Agilent Technologies foundation grant (to A. F. O. and M. S. C.).
[S] This article contains supplemental Tables 1 and 2.
[1] Supported by developmental funds from the Dept. of Cell Biology (University of Pittsburgh). To whom correspondence should be addressed: Dept. of Cell Biology, School of Medicine, S368 Biomedical Sciences Tower I, University of Pittsburgh, Pittsburgh, PA 15261. Tel.: 650-521-1032; Fax: 412-648-8330; E-mail: allyod@pitt.edu.
[2] Present address: School of Life Sciences, Tsinghua University, Beijing 100084, China, and Graduate School at Shenzhen, Tsinghua University, Shenzhen 518055, China.
[3] To whom correspondence should be addressed: Dept. of Biology, 337 Campus Dr. West, Stanford University, Stanford, CA 94305-5020. Tel.: 650-723-9970; Fax: 650-724-9945; E-mail: mcyert@stanford.edu.

[4] The abbreviations used are: GPCR, G-protein-coupled receptor; AzC, azetidine 2-carboxylic acid; CN, calcineurin/PP2B; Can, canavanine; Gal4-DBD, Gal4 DNA-binding domain; Gal4-TAD, Gal4 transcriptional activation domain; MIN, minimal medium; PM, plasma membrane; SC, synthetic complete medium; WCE, whole cell extract; ANOVA, analysis of variance; CHX, cycloheximide; G6PD, glucose-6-phosphate dehydrogenase; CIP, calf intestinal alkaline phosphatase.

that link Rsp5 to specific membrane proteins and also directly interact with the trafficking machinery, such as clathrin adaptor complexes, to promote cargo trafficking (15, 24). In mammals, α-arrestins associate with Nedd4, contribute to down-regulation of GPCR signaling, and impact the capacity for nutrient uptake (specifically glucose) (26–30). Recent reports also implicate ArrDC3 and Nedd4 in endocytosis of β4 integrin in breast cancer cells and demonstrate that another mammalian ArrDC TXNIP (also known as VDUP1 for vitamin D_3 up-regulated protein-1) promotes clathrin-mediated endocytosis of the glucose transporter GLUT1 (31, 32). Therefore, regulation of endocytosis is likely a conserved function of α-arrestins.

Importantly, α-arrestin-mediated trafficking is both signal- and cargo-selective. Some transporters seem to associate with a single dedicated α-arrestin, whereas others can recruit multiple arrestins. Many α-arrestins regulate several different transporters, and the α-arrestin-cargo association can change depending on the signal inducing internalization (12, 20, 33). For example, in yeast α-arrestin Ldb19/Art1 regulates endocytosis of the lysine permease Lyp1 in response to excess lysine, whereas α-arrestin Ecm21/Art2 regulates Lyp1 internalization in response to general stress (20).

How do α-arrestins achieve this signal-induced cargo selectivity? Recent reports suggest that phosphorylation blocks α-arrestin-mediated endocytosis and, conversely, that dephosphorylation releases this inhibition (17, 34, 35). For example, Art1-mediated endocytosis of the arginine permease Can1 is impaired when Art1 is phosphorylated by Npr1 (34), a kinase that is activated during nitrogen starvation, a condition known to inhibit permease internalization (35–37). Similarly, in response to nitrogen starvation, Npr1-dependent phosphorylation of Bul1 and Bul2, recently identified as yeast α-arrestins, impairs Bul-mediated endocytosis of the general amino acid permease Gap1 (35). In addition, phosphorylation of α-arrestin Rod1/Art4 by Snf1 (mammalian ortholog is the AMP- and ADP-activated protein kinase) blocks its ability to internalize the lactic acid permease Jen1, whereas dephosphorylation of Rod1 promotes endocytosis of Jen1 (17). In mammalian cells similar phospho-inhibition was recently demonstrated; phosphorylation of α-arrestin TXNIP by AMP- and ADP-activated protein kinase induces α-arrestin degradation, thereby impeding endocytic turnover of the glucose transporter GLUT1 (32). Hence, identification of the kinases and phosphatases that modify α-arrestins provides important mechanistic insights into the regulation of α-arrestin-mediated trafficking. Although dephosphorylation of at least some α-arrestins appears to be required for their function in permease endocytosis, direct dephosphorylation by a specific phosphatase has not yet been shown for any α-arrestin.

One signal-regulated phosphatase that is a good candidate for α-arrestin regulation is calcineurin (also called phosphoprotein phosphatase 2B or PP2B), a calcium and calmodulin-dependent phosphoprotein phosphatase conserved across eukaryotes and the target of the immunosuppressant drugs, FK506 and cyclosporin A. In mammals, calcineurin is abundant in the brain, where it regulates synaptic vesicle endocytosis, neural outgrowth, and synaptic plasticity; in other tissues, it impacts a wide range of processes, playing critical roles in T-cell differentiation and muscle development (38, 39). Although not essential in yeast under standard growth conditions, calcineurin is required for survival under various stressful conditions, such as in the presence of high salt, at alkaline pH, or in the presence of cell wall perturbants (40). Calcineurin promotes survival under stress conditions by binding to substrates that contain a conserved docking motif (P*X*I*X*IT and variants thereof) (39, 41) and dephosphorylating these targets to facilitate their function in stress adaptation. For example, dephosphorylation of the transcription factor Crz1 in response to cell wall stress induces expression of cell wall maintenance genes (42), whereas dephosphorylation of Hph1, an endoplasmic reticulum resident protein involved in protein translocation, assists in adaptation to alkaline pH (43, 44). In this regard, the first indication that calcineurin might also regulate endocytosis in yeast was the observation that calcineurin dephosphorylates two plasma membrane-localized phosphatidylinositol 4,5-bisphosphate-binding proteins (Slm1 and Slm2) to promote heat-induced internalization of the uracil permease Fur4 (45).

Here, we show that α-arrestin Aly1/Art6 is a new substrate of calcineurin and demonstrate that dephosphorylation of Aly1 by calcineurin is required for Aly1-mediated internalization and delivery to the vacuole of a nutrient permease. Aly1/Art6 and its closely related paralog Aly2/Art3 regulate intracellular sorting of the general amino acid permease Gap1 in response to nitrogen supply (24). Aly2 also promotes endocytosis of the aspartic acid/glutamic acid permease Dip5, a function that Aly1 was suggested, but not previously shown, to share (18). We located 22 phospho-sites in Aly1, identified a subset of these as regulated by calcineurin, and delineated the specific P*X*I*X*IT-docking motif in Aly1 needed for its interaction with and dephosphorylation by calcineurin. We further show that Aly1 mutants that cannot be dephosphorylated by calcineurin or that mimic persistent phosphorylation are unable to reduce cell surface levels of Dip5. Thus, these studies identify a new role for calcineurin in membrane trafficking; calcineurin promotes vacuolar trafficking of Dip5 by dephosphorylating Aly1, thereby stimulating its endocytic function. By contrast, we found that dephosphorylation of Aly1 is not required for its role in the intracellular sorting of Gap1. Our data add to the growing body of evidence that α-arrestin-mediated trafficking is strictly controlled by a phosphorylation-dependent switch wherein phosphorylation blocks and dephosphorylation promotes the function of an α-arrestin in endocytosis. This study further identifies the first phosphatase responsible for direct regulation of an α-arrestin.

EXPERIMENTAL PROCEDURES

Yeast Strains and Growth Conditions—Yeast strains used in this study and their construction are described in supplemental Table 1 (84, 85). Synthetic complete (SC) medium was prepared as in Refs. 24, 46 with 2.5 g/liter $(NH_4)_2SO_4$ used routinely as the nitrogen source. Minimal (MIN) medium was made in the same way as SC, except that only the amino acids required for growth of auxotrophic strains were provided. Cells were grown at 30 °C unless otherwise indicated. For growth assays on agar plates, 5-fold serial dilutions of stationary phase cultures with a starting density of $\sim 1 \times 10^7$ cells/ml were plated onto the indi-

cated medium and grown for 3–6 days at 30 °C. Rapamycin (LC Laboratories, Woburn, MA), azetidine 2-carboxylic acid (AzC) (Sigma), and canavanine (Can) (Sigma) were added to either SC or MIN + 0.5% $(NH_4)_2SO_4$ at the concentrations indicated. Yeast two-hybrid analyses employed yeast strain PJ69-4a (47) containing pGBT9-derived plasmids bearing Gal4 DNA-binding domain (DBD) fusions and pACT2-derived plasmids bearing Gal4 transcriptional-activation domain (TAD) fusions. Transformants were plated as serial dilutions onto SC medium lacking leucine and tryptophan, as a positive control for cell growth, or additionally lacking histidine or adenine, where growth is a read-out of *GAL1prom-HIS3* or *GAL2prom-ADE2* reporter activation, respectively. A competitive inhibitor of His3, 3-aminotriazole (Sigma), was added where indicated to the SC medium lacking histidine to increase the amount of *GAL1prom-HIS3* reporter expression needed to allow growth. Yeast cells were transformed using the lithium-acetate method (48).

Plasmids and DNA Manipulations—Plasmids used in this study and their construction, where applicable, are described in supplemental Table 2 (86–90). Plasmids were generated using standard recombinant DNA methods (49) and propagated in *Escherichia coli* strain DH5α. Site-directed mutagenesis, used to generate Aly1 plasmids with altered CN-binding sites or mutated serines/threonines, was performed with either the QuikChange II site-directed mutagenesis kit (Agilent Technologies, Santa Clara, CA) or using a similar methodology with Phusion high fidelity DNA polymerase (New England Biolabs, Ipswich, MA) and appropriately mutated primers. All constructs generated by PCR were verified using Sanger sequencing (50).

Yeast Protein Extraction, Purification, and Immunoblotting—Yeast protein extracts were generated by growing cells to mid-exponential phase at 30 °C ($A_{600\ nm}$ = 0.5–1.0) and harvesting an equal number of cells by centrifugation. In some cases, cell cultures were pretreated with either 2 μg/ml FK506 (LC Laboratories) for 30 min to inhibit CN or with 200 mM calcium chloride for 10 min to stimulate CN-mediated dephosphorylation. Cells were then lysed using sodium hydroxide, and proteins were precipitated using trichloroacetic acid (TCA) (51). Precipitated protein was solubilized by resuspension in SDS/-urea sample buffer (40 mM Tris (pH 6.8), 0.1 mM EDTA, 5% SDS, 8 M urea, and 1% β-mercaptoethanol) and heating to 37 °C for 15 min. An equal amount of extract was resolved by SDS-PAGE and specific proteins identified by immunoblotting (for a list of antibodies used see below). Immunoblotting with anti-Pgk1, anti-Pma1, or anti-Zwf1 (glucose-6-phosphate dehydrogenase, hereafter referred to as G6PD) was used to assess protein loading.

To assess Dip5-GFP stability, MKY1800 (*aly1*Δ *aly2*Δ *DIP5-GFP*) cells containing pRS315, pRS315-Aly1, pRS315-Aly1$^{\Delta PILKIN}$, pRS315-Aly2, pRS315-Aly1^{5E}, or pRS315-Aly1^{5A} were grown to mid-exponential phase at 30 °C in MIN + 0.5% $(NH_4)_2SO_4$ and treated with 200 μg/ml aspartic acid and glutamic acid to trigger Dip5 endocytosis. Cell samples were taken at times indicated post-aspartic/glutamic acid addition, and total protein was extracted using the sodium hydroxide lysis and TCA precipitation method described above. Dip5-GFP signal intensity, normalized for loading using G6PD, was quantified using ImageJ (National Institutes of Health), and the percentage of Dip5 remaining at each time point post-aspartic acid/glutamic acid addition was plotted. A representative data set from at least three independent experiments is shown.

Yeast extracts for pulldowns using GST fusion proteins were prepared by growing either strain BJ5459 or JR11 containing the pKK212-derived Aly1 or Aly2 expression plasmid indicated to mid-exponential phase in SC medium lacking tryptophan and inducing expression of *CUP1* promoter-driven GST or GST-Aly fusions with 200 μM $CuSO_4$ for 60 min. Where indicated, cells were also treated with either FK506 or $CaCl_2$ as described above. Cells were harvested by centrifugation, washed, frozen in liquid N_2, and stored at −80 °C. Cell pellets were then resuspended in co-IP buffer (50 mM Tris-HCl (pH 7.4), 15 mM EGTA, 100 mM NaCl, 0.2% Triton X-100, 5 mM *N*-ethylmaleimide, with phosphatase inhibitors (5 mM NaF, 5 mM Na_2MoO_4, 5 mM EDTA, 5 mM EGTA, 1 mM sodium orthovanadate, 2.5 mM β-glycerophosphate, 10 mM sodium pyrophosphate, and 0.4 mM sodium metavanadate), and protease inhibitors (Complete protease inhibitor mixture tablets, Roche Applied Science)) and lysed at 4 °C using glass beads and vigorous vortexing. GST fusion proteins were purified from equal concentrations of clarified lysates by incubation with glutathione-Sepharose beads (GE Healthcare). Pulldowns were washed three times in 500 μl of co-IP buffer, aspirated to dryness, eluted in Laemmli buffer (52), resolved by SDS-PAGE, and assessed by immunoblotting. GST-Aly1 proteins treated with calf intestinal alkaline phosphatase (CIP) (New England Biolabs) were purified as described above, washed with CIP buffer, and incubated with 30 units of CIP for 30 min at 37 °C prior to elution in Laemmli buffer (52) and further analyses.

Where indicated, immunoblots were probed with the following: rabbit polyclonal anti-GST (Sigma); mouse monoclonal anti-GFP (Covance, Emeryville, CA); rabbit polyclonal anti-GFP (Molecular Probes, Carlsbad, CA); rabbit polyclonal anti-HA (Covance); mouse monoclonal anti-ubiquitin (gift from Richard Gardner, University of Washington, Seattle); rabbit polyclonal anti-Bmh (recognizes yeast 14-3-3 proteins Bmh1 and Bmh2; gift from Sandra Lemmon, University of Miami, FL); rabbit polyclonal anti-Rsp5 (gift from Linda Hicke, University of Texas, Austin); rabbit polyclonal anti-Pma1 (gift from Amy Chang, University of Michigan, Ann Arbor); rabbit polyclonal anti-Zwf1/G6PD (Sigma); and rabbit polyclonal anti-Pgk1 (53). Antibodies against Pma1, G6PD, or Pgk1 were examined to ensure equivalent loading of extracts. For all immunoblot data presented, anti-mouse and anti-rabbit secondary antibodies conjugated to IRDye-800 or IRDye-680 (Li-Cor Biosciences, Lincoln, NE) were detected using an Odyssey™ infrared imaging system (Li-Cor Biosciences). Quantification of immunoblots was performed using ImageJ 1.39u software (National Institutes of Health, Bethesda).

In Vitro Dephosphorylation Assays—GST-fused Aly1, Aly1$^{\Delta PILKIN}$, Aly2, and Crz1 were purified on glutathione-Sepharose beads from BJ5459 cell extracts as described above. Under these conditions, GST-arrestins purify with several

interacting proteins (24), including protein kinases.[5] To allow *in vitro* phosphorylation (and radiolabeling) of arrestins by these copurifying protein kinases, bead-bound proteins were washed and resuspended in "kinase" buffer (50 mM Tris-HCl (pH 7.5), 10 mM $MgCl_2$, 0.1 mM DTT, 0.1 mM unlabeled ATP, aprotinin, and leupeptin) and incubated at 30 °C for 60 min in the presence of 75 nM [γ-^{32}P]ATP (PerkinElmer Life Sciences). Unincorporated ^{32}P and copurifying proteins were removed from the glutathione-immobilized arrestins by repeated washing of beads with co-IP buffer containing an additional 650 mM NaCl, 2 mM EDTA, and 0.8% Triton X-100. Bead-bound proteins were then resuspended in kinase buffer (listed above) with either λ-phosphatase (New England Biolabs) or recombinant CN-trunc, a mutant version of calcineurin that lacks its autoinhibitory domain (which is constitutively active in the absence of calcium and calmodulin), and incubated at 30 °C. Samples were removed at the times indicated, beads were aspirated to dryness, and bound proteins were eluted in Laemmli buffer (52) and resolved by SDS-PAGE. Gels were stained with Gel Code Blue (Thermo Scientific), dried, exposed to a PhosphorImager™ screen, and imaged with a Typhoon scanner (GE Healthcare). ImageJ software was used to quantify changes in ^{32}P signal intensity (normalized for protein loading using quantification of Gelcode Blue staining) after incubation with phosphatase. Data were quantified from three replicates (representative data show), and the mean percentage of the original phosphorylation signal is plotted ± S.E.

Mass Spectroscopy Analysis—GST-fused Aly1 or Aly1$^{\Delta PILKIN}$ was purified from BJ5459 cells that were treated with either $CaCl_2$ (to stimulate calcineurin-mediated dephosphorylation) or FK506 (to block calcineurin-mediated dephosphorylation), as described above. Samples were resolved by SDS-PAGE and stained with Gelcode Blue (Thermo Scientific), and the bands corresponding to Aly1 or Aly1$^{\Delta PILKIN}$ were excised. Proteins in each gel slice were then trypsinized and extracted as described in the "Enzymatic Digestion of Proteins from Gel Bands" protocol provided by the California Institute for Quantitative Biosciences. Mass spectrometry of extracted peptides was performed by the Vincent J. Coates Proteomics/Mass Spectrometry Laboratory at University of California at Berkeley. A nano-LC column was packed in a 100-μm inner diameter glass capillary with an emitter tip. The column consisted of 10 cm of Polaris c18 5 μm packing material (Varian), followed by 4 cm of Partisphere 5 SCX (Whatman). The column was loaded by use of a pressure bomb and washed extensively with buffer A (see below). The column was then directly coupled to an electrospray ionization source mounted on a Thermo-Fisher LTQ XL linear ion trap mass spectrometer. Data collection was programmed so that neutral loss of phosphate would trigger the collection of an MS3 spectrum of the neutral loss peak. An Agilent 1200 HPLC equipped with a split line so as to deliver a flow rate of 30 nl/min was used for chromatography. Peptides were eluted using a four-step MudPIT procedure (54). Buffer A was 5% acetonitrile, 0.02% heptafluorobutyric acid; buffer B was 80% acetonitrile, 0.02% heptafluorobutyric acid. Buffer C was 250 mM ammonium acetate, 5% acetonitrile, 0.02% heptafluorobutyric acid; buffer D was same as buffer C but with 500 mM ammonium acetate. The programs SEQUEST and DTASELECT were used to identify peptides and proteins from a database composed of the Aly1 sequence and common contaminant proteins. A minimum XCORR of 1.5, 2.2, and 3.5 was required for charge states 1, 2, and 3, respectively. To assess enrichment of phosphorylated peptides in FK506-treated *versus* Ca^{2+}-treated samples, two-tailed Z-tests were preformed, and *p* values are reported in Table 1.

Uptake of ^{14}C-Labeled Amino Acids—Citrulline uptake assays were performed as described previously (24, 55). In brief, BY4741 cells were made prototrophic by transformation with pCK283 (56) and either pRS426, pRS426-Aly1, pRS426-Aly2, or pRS426-Aly1$^{\Delta PILKIN}$. Cells were grown to early exponential phase (~3–4 × 10^6 cells/ml) in MIN + 0.5% $(NH_4)_2SO_4$ medium, collected, washed by filtration, and resuspended in nitrogen-free medium, and 20 μM [^{14}C]citrulline (PerkinElmer Life Sciences) was added to cells to initiate uptake assays. Cell aliquots were removed every 30 s over four time points, collected, washed by filtration, and [^{14}C]citrulline incorporation was measured using a Beckman Coulter LS6500 Multipurpose Scintillation Counter (Indianapolis, IN). Multiple replicate assays were performed (minimum of three), and the rate of citrulline uptake (dpm/min/$A_{600\ nm}$) was determined. Aspartic acid uptake assays were performed as described for the citrulline uptake assays with the exception that 40 μM [^{14}C]aspartic acid (PerkinElmer Life Sciences) was employed to initiate the uptake assays. In each case, plotted data represent the rate of amino acid uptake relative to the wild-type control.

Fluorescence Microscopy—Cell imaging of MKY1800 (*aly1*Δ *aly2*Δ *DIP5-GFP*) containing pRS315, pRS315-Aly1, pRS315-Aly1$^{\Delta PILKIN}$, pRS315-Aly2, pRS315-Aly1^{5E}, or pRS315-Aly1^{5A} was performed at the Center for Biological Imaging (Pittsburgh, PA) using an Olympus IZ81 inverted microscope (Olympus America Inc., Center Valley, PA) with a 100 × 1.40 NA objective, and images were captured using a QImaging Retiga EXi CCD camera (QImaging, Surrey, British Columbia, Canada) and MetaMorph 7.5 Imaging System software (Molecular Devices, Sunnyvale, CA). Exposure times and microscope settings were kept constant during Dip5-GFP imaging. All Dip5-GFP images presented were processed equivalently using Adobe Photoshop software where intensity levels were adjusted and an unsharp mask filter applied (radius of 5 pixels). Pixel intensity for Dip5-GFP at the plasma membrane (PM) was measured by outlining PMs manually using a 3-pixel wide stroke with ImageJ software (National Institutes of Health) for a minimum of 140 cells per sample. Mean background fluorescence for each image was subtracted from the mean pixel intensity for each region of interest. The mean PM intensity (in arbitrary units) for each sample is plotted ± S.E., and statistical significance of changes in PM intensity was assessed using one-way ANOVA and Tukey's post hoc test using Prism software (GraphPad Software Inc., San Diego). To assess the ratio of PM to vacuolar fluorescence, PM intensities were determined as defined above, and each cell was assigned a specific number identifier. Vacuolar regions of interest were assigned using the corresponding differential interference contrast images and

[5] A. F. O'Donnell, R. G. Gardner, and M. S. Cyert, unpublished observations.

TABLE 1

Aly1 phosphopeptides identified by LC-MS^3

For each treatment, numbers indicate the number of phosphorylated peptides identified over the total number of peptides identified for that region. Phospho means phosphorylated. Note: in addition, Ser-188, Ser-214, Ser-215, Ser-216, Ser-220, Ser-228, and Ser-568 were identified as phosphorylated in PhosphoPep. Two-tailed Z-tests were used to assess the significance of differences in phosphorylated peptide populations between Ca^{2+}- and FK506-treated samples for both Aly1 and Aly1$^{\Delta PILKIN}$, and the *p* values from these tests are presented below. Tests results are significant if $p < 0.05$. If less than 30 total peptides were identified for a given region, the Z-tests were not determined (ND) as the sample size is prohibitively small for this analysis. If no phosphorylated peptides were identified in a particular comparison, the Z-test comparison is not applicable (NA). Green highlighting identifies the phospho-sites significantly enriched in Aly1 FK506-treated samples compared with Aly1 Ca^{2+}-treated samples based on Z-test analyses (*p* values listed). It should be noted that there are approximately 5-fold fewer total peptides identified for the Ca^{2+}-treated Aly1$^{\Delta PILKIN}$ compared with the FK506-treated Aly1$^{\Delta PILKIN}$ in these regions, which confounds comparison of enrichment in phosphorylation at these sites for Aly1$^{\Delta PILKIN}$. However, the enrichment for wild-type Aly1 between Ca^{2+} and FK506 treatments is apparent, and these same sites are heavily modified in the FK506-treated Aly1$^{\Delta PILKIN}$ samples as well. The four serines and one threonine mutated to alanine to generate Aly1^{5A} or glutamic acid to generate Aly1^{5E} are underlined.

Aly1 phospho-site	Aly1 + Ca^{2+} (phospho. /total)	Aly1 + FK (phospho. /total)	Z-test p-values Aly1 + Ca^{2+} vs Aly1 +FK	Aly1$^{\Delta PILKIN}$ + Ca^{2+} (phospho. /total)	Aly1$^{\Delta PILKIN}$ + FK (phospho. /total)	Z-test p-values Aly1$^{\Delta PILKIN}$ + Ca^{2+} vs Aly1$^{\Delta PILKIN}$ +FK	Identified in Phospho Pep	Identified in Phospho GRID	Conser-ved in other fungi?
T54	1/113	0/50	0.502	0/60	0/70	NA	No	No	No
S154	0/105	1/205	0.472	0/62	0/204	NA	No	No	Yes
S157	0/105	1/205	0.472	0/62	0/204	NA	No	No	Yes
S174	1/69	0/230	0.067	0/64	0/90	NA	No	No	Yes
S182	0/68	1/64	0.303	1/164	0/207	0.263	No	No	Yes
S184	3/68	3/64	0.936	2/164	10/207	0.051	Yes	Yes	No
S185	1/68	0/64	0.332	1/164	0/207	0.263	Yes	No	Yes
T210	0/17	1/4	ND	0/32	2/12	ND	Yes	No	No
T250	0/121	0/152	NA	0/13	1/117	ND	No	No	Yes
S252	0/121	20/152	0.000	0/13	32/117	ND	No	No	No
***S568**	0/55	0/76	NA	0/30	0/168	NA	Yes	No	No
S569	1/55	4/76	0.308	0/30	10/168	0.171	Yes	No	Yes
S573	2/55	25/76	0.000	0/30	17/168	0.069	Yes	No	Yes
S585	5/26	4/43	0.234	0/28	29/130	ND	No	No	No
T768	2/165	0/98	0.276	0/47	4/70	0.095	No	No	No
S786	1/203	1/480	0.529	1/204	2/234	0.646	No	No	No
T790	1/203	0/480	0.124	0/204	2/234	0.189	No	No	No
S791	1/203	0/480	0.124	0/204	1/234	0.352	No	No	No
S813	3/666	0/337	0.219	0/79	0/319	NA	Yes	No	No
S814	1/666	0/337	0.478	0/79	0/319	NA	Yes	No	No
S824	0/125	0/69	NA	0/89	3/50	0.019	Yes	No	Yes
S843	0/3	0/2	NA	0/19	1/1	ND	No	No	No
S883	0/19	0/23	NA	0/10	1/7	ND	No	No	No

* This denotes Ser-568, which was not identified as phosphorylated in our dataset but is close to other calcineurin-regulated sites and is phosphorylated in PhosphoPep and so was mutated in our analyses.

then overlaid onto the fluorescent images. Only cells where clear vacuolar morphology was evident on the differential interference contrast image were used in subsequent analyses. A minimum of 40 cells was assessed this way per sample, and the mean PM/vacuolar fluorescence intensity is presented. Error bars represent ± S.E. and statistical significance of changes in PM/vacuolar fluorescence intensity ratio assessed using one-way ANOVA and Tukey's post hoc test in Prism software.

RESULTS

C-terminal PXIXIT Motif in Aly1 Mediates Its Association with Calcineurin—Yeast two-hybrid analysis successfully identified several calcineurin substrates (43, 45, 57, 58). To identify additional potential substrates, we conducted a yeast two-hybrid screen using a Gal4-DBD fusion to Cna1, a catalytic subunit of calcineurin, as the bait. The plasmid that showed the strongest interaction with this bait encoded the C-terminal half (amino acids 493–915) of Aly1 fused in-frame to the Gal4-TAD (Fig. 1*A*). Further yeast two-hybrid analysis using the PJ69-4a reporter strain (47) revealed that full-length Aly1 interacts with yeast Cna1 (Fig. 1, *A* and *B*) and even with the catalytic subunit (CNA) of *Homo sapiens* calcineurin (Fig. 1*B*). Neither yeast Cna1 nor human CNA interacted with Aly2, the Aly1 paralog (39% identity; 64% similarity), or with any other yeast α-arrestin (Fig. 1*B*), even though every α-arrestin tested was expressed in the yeast two-hybrid strain (Fig. 1*C*).

The original library screen identified residues 493–915 of Aly1 as sufficient for robust interaction with Cna1 (Fig. 1*A*). To narrow down the region of Aly1 that interacts with calcineurin, various deletions and truncations were tested using the same yeast two-hybrid method. An even shorter segment of the C-terminal portion of Aly1, residues 610–915, was sufficient for Cna1 binding. Further truncations established that Aly1 residues 822–915, but not 838–915 or 610–831, interacted with Cna1 (Fig. 1*A*), suggesting that the residues responsible for the Aly1-Cna1 association are contained within amino acids 831–838. Indeed, residues 832–837 correspond to PILKIN, a sequence related to the consensus P*X*I*X*IT-docking motif found in many calcineurin substrates (43, 45, 59–62). As a critical test of the role of this sequence element, a precise 6-residue deletion (Aly1$^{\Delta PILKIN}$) was constructed and failed to interact with Cna1 (Fig. 1*B*), even though it was expressed (as a Gal4-

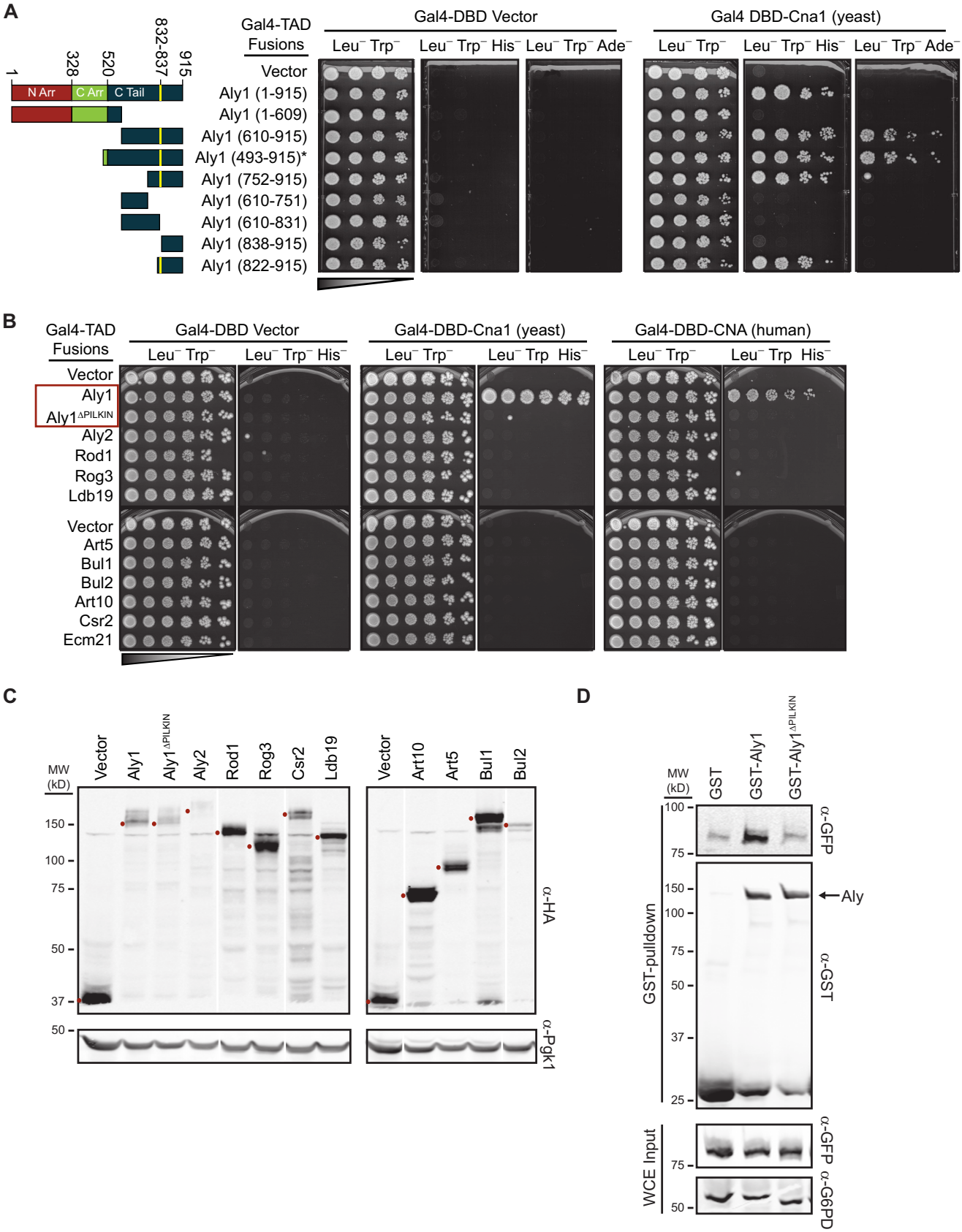

TAD-fusion) at a level equivalent to the wild-type Aly1 fusion (Fig. 1*C*).

To confirm that the interaction detected by the yeast two-hybrid method is physiologically relevant, we overexpressed either GST alone or fused to Aly1 or Aly1$^{\Delta PILKIN}$ from the copper-inducible promoter *CUP1* in yeast cells coexpressing GFP-tagged Cna1 from its chromosomal locus. Reassuringly, Cna1-GFP strongly associated with Aly1 but did not associate with Aly1$^{\Delta PILKIN}$ at a level any higher than seen with the negative control (GST alone) (Fig. 1*D*), demonstrating that Aly1 interacts with calcineurin *in vivo* and that this interaction requires the PILKIN motif near the C-terminal end of Aly1.

Aly1 Is a Substrate of Calcineurin—Next, we tested whether Aly1 was dephosphorylated by calcineurin *in vitro*. For many calcineurin substrates, loss of the P*X*I*X*IT-docking motif abrogates phosphatase binding and prevents dephosphorylation (43, 45, 59, 60). To prepare phosphorylated versions of Aly1, Aly1$^{\Delta PILKIN}$ (lacks the calcineurin-binding site), and Aly2 (does not bind calcineurin), we purified these proteins (as GST fusions) from yeast under low stringency conditions to retain associated protein kinases. Indeed, when these preparations were incubated with [γ-^{32}P]ATP, radioactivity was readily incorporated into all three proteins but not into the GST alone control purified in the same fashion (data not shown). After stringent washing to remove the kinases and unincorporated [γ-^{32}P]ATP, the radiolabeled proteins were then incubated with either purified calcineurin or λ-phosphatase (Fig. 2*A*, *t = 0 lanes*). Recombinant Crz1, a known calcineurin substrate (60, 61), radiolabeled by phosphorylation with protein kinase Hrr25 (63), was used as a positive control. Upon incubation with calcineurin, both Aly1 and Crz1, but neither Aly1$^{\Delta PILKIN}$ nor Aly2, exhibited the increased electrophoretic mobility and decreased ^{32}P label indicative of dephosphorylation (Fig. 2, *A* and *B*), whereas all four substrates were dephosphorylated by λ-phosphatase (Fig. 2*A*). Thus, Aly1, but not Aly2, is a direct substrate for calcineurin *in vitro*, and the PILKIN sequence, which represents the P*X*I*X*IT motif in Aly1, is required for calcineurin to interact with and dephosphorylate Aly1.

Calcineurin Dephosphorylates a Specific Subset of Phospho-sites in Aly1—We noted that calcineurin-mediated dephosphorylation of Crz1, a substrate with a high affinity for calcineurin, was more rapid and complete than dephosphorylation of Aly1 (Fig. 2*A*; compare *t* = 30 min for Aly1 and Crz1). Incubation of Crz1 with either calcineurin or λ-phosphatase resulted in a similar shift in electrophoretic mobility and equivalent loss of ^{32}P signal. In contrast, Aly1 was not dephosphorylated as extensively by calcineurin as it was by λ-phosphatase (Fig. 2*A*), suggesting that only a subset of Aly1 phospho-sites are regulated by calcineurin.

To assess whether Aly1 is a calcineurin substrate *in vivo*, we examined the electrophoretic mobility of Aly1 or Aly1$^{\Delta PILKIN}$ extracted from yeast treated with the following: (*a*) FK506, which inhibits calcineurin (64); (*b*) Ca^{2+}, which stimulates calcineurin; or (*c*) a combination of FK506 followed by Ca^{2+}, to control for any Ca^{2+}-stimulated calcineurin-independent effects. Similar analyses were conducted with Aly1^{PVIVIT}, a mutant in which PILKIN was converted to a known P*X*I*X*IT variant that displays high affinity calcineurin binding (59, 65), and with Aly1^{AAAAAA}, in which the PILKIN sequence was abrogated by six Ala substitution mutations. Upon calcineurin activation, only Aly1 and Aly1^{PVIVIT} migrated as a discrete doublet with the faster migrating band (below the 150-kDa marker) distinctly more prevalent than the slower migrating species (above the 150-kDa marker) (Fig. 2*C*). In contrast, Aly1$^{\Delta PILKIN}$ and Aly1^{AAAAAA} exhibited a diffuse banding pattern even when calcineurin was activated (Fig. 2*C*, compare Ca^{2+}-treated lanes). The same diffuse banding pattern was displayed by all versions of Aly1 when calcineurin was inhibited by treating cells with FK506 (Fig. 2*C*), consistent with a lack of dephosphorylation and a concomitant increase in phospho-Aly1 isoforms.

In agreement with this conclusion, a diffuse Aly1 migration pattern was also observed in cells where calcineurin activity was abolished by other means, specifically through loss of its regulatory subunit (in a *cnb1*Δ mutant) or loss of both of its catalytic subunits (a *cna1*Δ *cna2*Δ double mutant) (Fig. 2*D*). Moreover, in contrast to the effect observed in wild-type cells, in the absence of functional calcineurin the addition of Ca^{2+} failed to generate a defined Aly1 doublet with a prominent faster migrating species (Fig. 2*D*, compare *Ca-treated lanes*).

To confirm that the diffusely migrating species represent phosphorylated isoforms, purified GST-Aly1, Aly1$^{\Delta PILKIN}$, Aly1^{PVIVIT}, and Aly1^{AAAAAA} were treated with CIP. In all cases, treatment with CIP collapsed Aly1 species into a crisp doublet in which the fastest migrating band was markedly more prominent (Fig. 2*E*), demonstrating that the diffuse migration of the Aly1 doublet is due to phosphorylation. As observed *in vitro* (Fig. 2*A*), *in vivo* activation of calcineurin did not sharpen the Aly1 doublet to the same extent as incubation with CIP (Fig. 2*E*, compare Ca^{2+}-treated Aly1 or Aly1^{PVIVIT} −/+ CIP), further suggesting that calcineurin is responsible for dephosphorylation of only a subset of phospho-sites in Aly1.

Calcineurin-mediated Dephosphorylation Does Not Influence Aly1 Ubiquitinylation or Stability—Because Aly1 was identified as an *in vitro* substrate for the ubiquitin ligase Rsp5 (66), the GST-Aly1 species isolated from cell extracts was probed with an anti-GST antibody and an anti-ubiquitin antibody to allow simultaneous detection of ubiquitinylated and nonubiquitinylated forms on immunoblots. This analysis revealed that the slower migrating band in the Aly1 doublet is ubiquitinylated (band above 150-kDa marker; Aly1-Ub, Fig. 2, *C–E*). As noted above, both bands in the Aly1 doublet were sharpened upon addition of CIP (Fig. 2*E*), suggesting that both

FIGURE 1. **Aly1 interacts with the catalytic subunit of CN from both yeast and humans.** *A* and *B,* serial dilutions of PJ69-4a containing the indicated Gal4-TAD and Gal4-DBD fusions were plated on SC medium lacking the amino acids indicated and grown for 4 days at 30 °C. *A*, schematic depicting the region of Aly1 expressed as Gal4-TAD fusion is provided where the N-terminal arrestin-fold (*N Arr*), C-terminal arrestin-fold (*C Arr*), C-terminal tail (*C Tail*), and P*X*I*X*IT motif are shown in *red, green, blue* and *yellow,* respectively. *B*, *red box* helps to highlight the comparison between the full-length Aly1 and Aly1 missing the P*X*I*X*IT motif (PILKIN). *C,* expression of the indicated Gal4-TAD fusions in the two-hybrid reporter strain PJ69-4a was assessed by immunoblotting with anti-HA (Covance) after resolving TCA-extracted whole cell lysates (*WCE*) by SDS-PAGE. *Red dots* denote the full-length α-arrestin-Gal4-TAD fusion. *White lines* indicate removal of redundant replicate lanes. *D,* copurification of the catalytic subunit of CN, Cna1-GFP, with GST, GST-Aly1, or GST-Aly1$^{\Delta PILKIN}$ (expressed from pKK212-derived plasmids) from extracts of BJ5459 cells was assessed by immunoblotting. 1% of the whole cell lysates used as input for the pulldowns is shown.

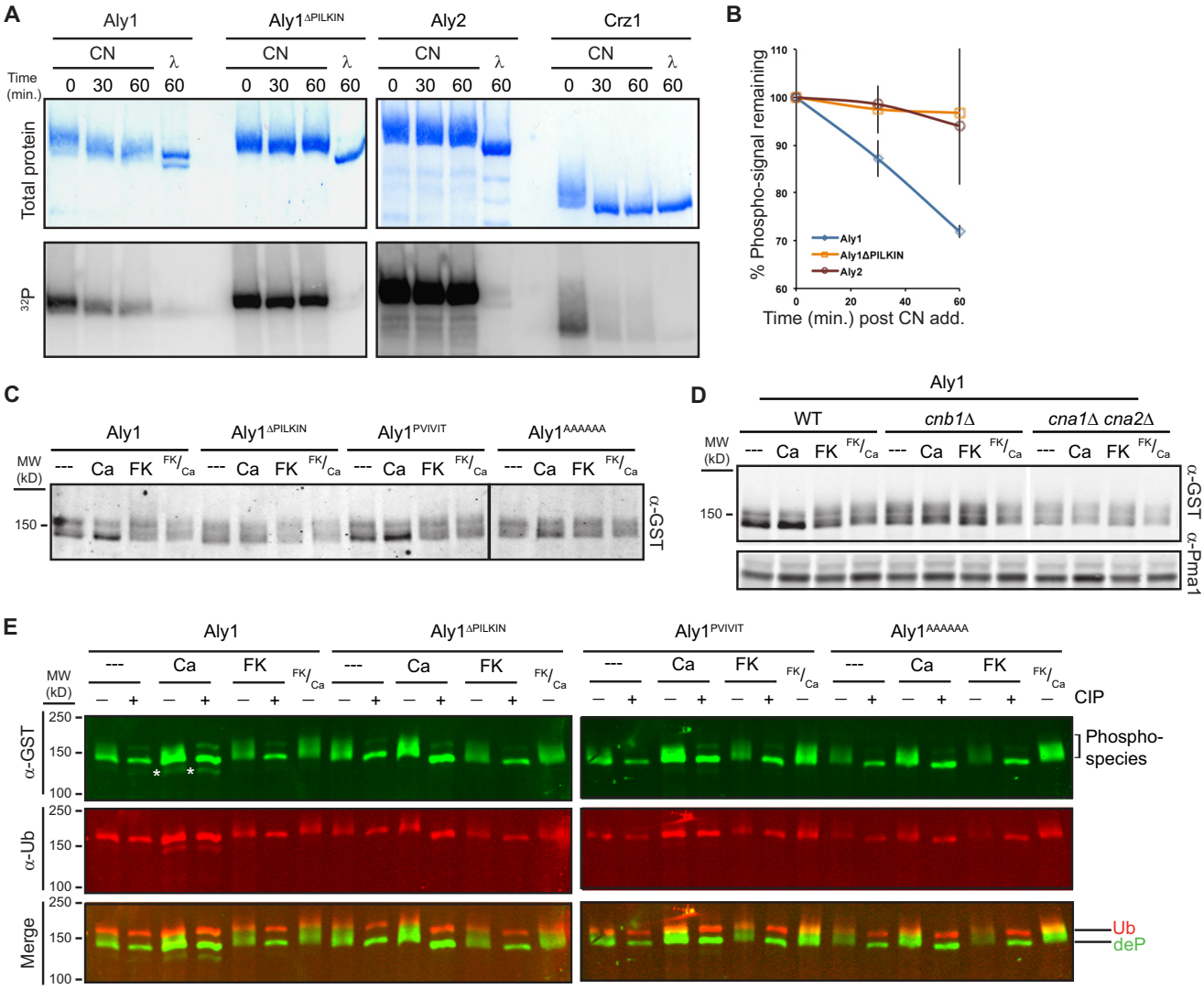

FIGURE 2. **Aly1, but not Aly1$^{\Delta PILKIN}$, is a CN substrate *in vitro* and *in vivo*.** *A,* GST-tagged Aly1, Aly1$^{\Delta PILKIN}$, Aly1, and Crz1 were purified on glutathione-Sepharose beads yeast extracts, incubated with [γ-^{32}P]ATP, and phosphorylated by copurifying kinases. Glutathione-bound proteins were washed to squelch further phosphorylation, incubated with CN-trunc or λ-phosphatase for the indicated times, and assessed by SDS-PAGE. Gels were stained for total protein or imaged to detect ^{32}P. Representative data from one of four replicates are shown. *B,* values plotted are the mean percent decrease in phospho-signal upon addition of CN-trunc (normalized for loading) for four replicate experiments performed as in *A,* and *error bars* represent the standard deviation of the means. *C,* BJ5459 cells expressing GST-Aly1, GST-Aly1$^{\Delta PILKIN}$ (a deletion of the CN-binding site), GST-Aly1^{PVIVIT} (a high affinity CN-binding site, Aly1^{PVIVIT}), or GST-Aly1^{AAAAAA} (mutation of the CN-binding site to alanines) were treated with nothing (−), 200 mM calcium chloride (*Ca*), 2 μg/ml FK506 (calcineurin inhibitor; *FK*), or a combination of FK506 followed by Ca ($^{FK}/_{Ca}$). WCEs generated by TCA extraction were resolved by on 4% acrylamide gels and assessed by immunoblotting. The *black line* between lanes in *C* indicates where samples were run on two separate gels. *D,* WCEs from cells treated as in *C* were TCA-extracted from BJ5459 cells lacking either the regulatory subunit of CN (*cnb1*Δ) or the two catalytic subunits of CN (*cna1*Δ *cna2*Δ). A *white line* indicates lane removal. *E,* treatment of GST-purified Aly1 and Aly1 mutants with calf intestinal alkaline phosphatase assists in identifying Aly1 phospho-species. BJ5459 cells expressing either GST-Aly1, GST-Aly1$^{\Delta PILKIN}$, GST-Aly1^{PVIVIT}, or GST-Aly1^{AAAAAA} (each expressed from pKK212-derived plasmids) were treated with nothing (−), Ca, FK, or both FK and Ca, and WCEs were made by glass bead lysis. GST-tagged arrestins were purified from these lysates and treated with calf intestinal alkaline phosphatase (+ *CIP*) or mock incubated in CIP buffer (− *CIP*) at 37 °C for 30 min. Arrestins were then resolved on 4% acrylamide gels and analyzed by immunoblotting using a Li-COR Odyssey imaging station, allowing for detection of both the anti-ubiquitin (*Ub*) antibody (with anti-mouse IRDye 680) and the anti-GST antibody (with anti-rabbit IRDye 800) simultaneously. The *white asterisks* denote a proteolysis product generated during protein extraction.

Aly1 and Aly1-Ub are phosphorylated. Importantly, there was no apparent defect in ubiquitinylation of Aly1 when the calcineurin-binding site was mutated or in response to altered calcineurin activity (Fig. 2*E*).

It has been reported that the phosphorylation status of yeast α-arrestins Bul1, Bul2, and Rod1 impacts their ubiquitinylation and/or interaction with Rsp5 (17, 35) and that phosphorylation regulates the stability of the mammalian α-arrestin, TXNIP (32). We therefore tested whether dephosphorylation of Aly1 by calcineurin affected any of these properties. Dephosphorylation of Aly1 by calcineurin did not alter Aly1 stability; in cells treated with Ca^{2+} to activate calcineurin and cycloheximide (CHX) to inhibit protein synthesis, the degradation profiles of Aly1 and Aly1$^{\Delta PILKIN}$ were indistinguishable (Fig. 3, *A* and *B*). Furthermore, neither ubiquitinylation of Aly1, nor its interaction with Rsp5 appeared to be regulated by calcineurin. Aly1 and Aly1$^{\Delta PILKIN}$ were both ubiquitinylated (Fig. 2*E*), and equivalent amounts of Rsp5 copurified with Aly1 and Aly1$^{\Delta PILKIN}$ from yeast extracts (Fig. 3*C*). As a control in these experiments, we included mutants (Aly1^{Y686G} or Aly2^{Y703G}) in which puta-

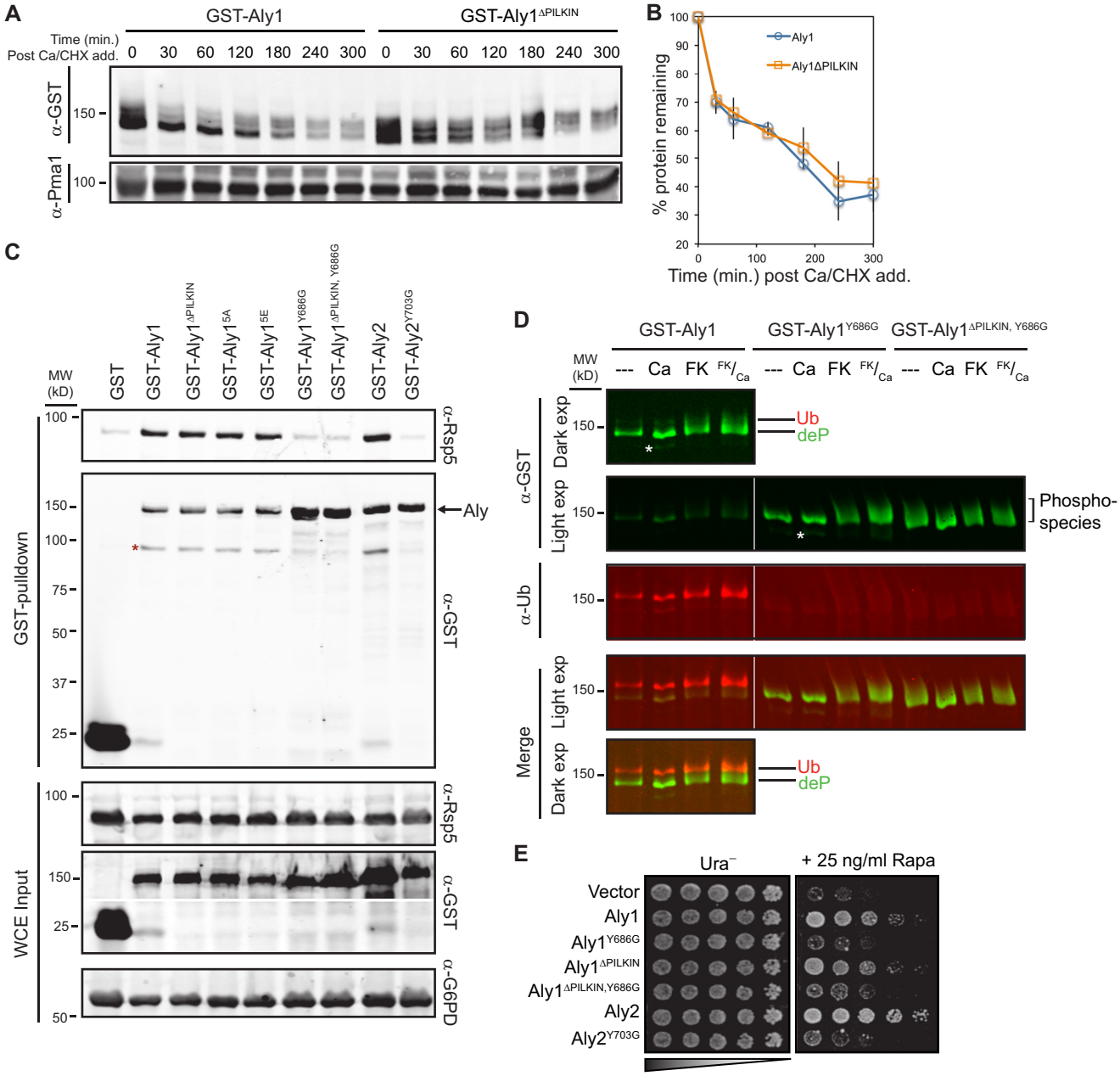

FIGURE 3. **CN regulation does not alter Aly1 stability or association with Rsp5.** *A,* BJ5459 cells expressing either GST-Aly1 or GST-Aly1$^{\Delta PILKIN}$ (from pKK212-derived plasmids) were treated with 200 mM calcium for 10 min (to stimulate CN activity and dephosphorylation of the WT Aly1 protein) and then incubated with 50 μg/ml CHX. Culture samples were removed at the times indicated post-CHX addition; WCEs were prepared by TCA extraction, and Aly1 mobility and levels were assessed on 4% acrylamide gels followed by immunoblotting. Representative data from three replicate experiments are shown. *B,* Aly1 and Aly1$^{\Delta PILKIN}$ protein levels (assessed as in *A*) were quantified, and the mean percentage of Aly1 or Aly1$^{\Delta PILKIN}$ protein remaining (three replicates, normalized for loading) after CHX addition is plotted with *error bars* representing ± S.D. *C,* GST, GST-Aly1, GST-Aly1$^{\Delta PILKIN}$, GST-Aly1^{5A}, GST-Aly1^{5E}, GST-Aly1^{Y686G}, GST-Aly1$^{\Delta PILKIN,Y686G}$, GST-Aly2, or GST-Aly2^{Y703G} (expressed from pKK212-derived plasmids) were extracted and purified using glutathione-Sepharose beads. Copurification of endogenous Rsp5 was assessed by immunoblotting. 4% of the WCE used as input for pulldowns is shown. A *red asterisk* denotes residual signal from the anti-Rsp5 antibody detection in the anti-GST pulldown blots. A *horizontal white line* denotes where the GST input blot has been cropped to conserve space. *D,* indicated GST fusions purified from cells treated with nothing (−), Ca, FK, or FK followed by Ca, resolved on 4% acrylamide gels, and immunoblotted for detection of ubiquitin (*Ub*) (with anti-mouse IRDye 680) and GST (anti-rabbit IRDye 800) simultaneously. The *white asterisks* denote a proteolysis product generated during protein extraction. For Aly1, both darker and lighter exposures are shown because the levels of Aly1 are significantly lower than those for the Y686G mutants. The darker exposure for wild-type Aly1 allows visualization of the calcineurin-dependent band shift and serves as a ubiquitinylated control for the Y686G mutant proteins. *E,* growth of serial dilutions of BY4741 cells containing pRS426 (vector), pRS426-Aly1, pRS426-Aly1^{Y686G}, pRS426-Aly1$^{\Delta PILKIN}$, pRS426-Aly1$^{\Delta PILKIN,Y686G}$, pRS426-Aly2, or pRS426-Aly1^{Y703G} on SC medium lacking uracil (Ura^{-} control medium) or SC-Ura^{-} with rapamycin.

tive Rsp5-binding sites in Aly1 or Aly2 (66) were changed from a canonical PP*X*Y motif to PP*X*G. Introducing these mutations into Aly1, Aly1$^{\Delta PILKIN}$, or Aly2 reduced the association of each protein with Rsp5 to the background levels observed with the GST control (Fig. 3*C*). In addition, introducing this mutation into Aly1 resulted in loss of ubiquitinylation and an increased level of this protein (Fig. 3, *C* and *D*). However, in contrast to Aly1, Aly1$^{\Delta PILKIN}$, and Aly2, whose overexpression confers

resistance to rapamycin, a TORC1 inhibitor that mimics nitrogen starvation (Fig. 3*E*) (24, 67), overexpression of PP*X*G mutant Aly alleles failed to improve growth under these conditions, suggesting that these mutations abrogate the function of these proteins *in vivo* (Fig. 3*E*). Thus, ubiquitinylation of Aly1 resulted in an observed, slower migrating form of the protein, and neither the ubiquitinylation, stability, nor ability of Aly1 to bind Rsp5 was altered by its calcineurin-mediated dephosphorylation.

Mapping of Calcineurin-regulated Phospho-sites in Aly1—To determine which residues of Aly1 are phosphorylated and which are susceptible to dephosphorylation by calcineurin, we performed LC-MS^3 analysis of purified GST-tagged Aly1 and Aly1$^{\Delta PILKIN}$ extracted from cells in which calcineurin was activated (by treatment with Ca^{2+}) or in which calcineurin was inhibited (by treatment with FK506). Peptides covering >50% of the protein were recovered (Fig. 4*A*), and a total of 22 phosphorylated residues in Aly1 were identified (Fig. 4*B* and Table 1), several of which were also earmarked as phospho-sites in various yeast global phosphoproteomic analyses (Table 1) (68, 69). Statistical analysis showed that of these 22 phospho-sites, two (Ser-252 and Ser-573) were significantly enriched in FK506-treated Aly1 (and also identified in FK506-treated Aly1$^{\Delta PILKIN}$), making them good candidate sites for regulation by calcineurin (Fig. 4*B* and Table 1). Two other sites (Thr-250 and Ser-569) near Ser-252 and Ser-573, respectively, occasionally showed a modest enrichment, and a fifth site, Ser-568, near Ser-573, although not detected in our work, was reported to be an *in vivo* phospho-site in PhosphoPep (66). All these sites (except Ser-568) fit an -(S/T)P- consensus, and all lie in predicted solvent-exposed regions. Thus, based on these analyses, we mutated five candidate sites (Thr-250, Ser-252, Ser-568, Ser-569, and Ser-573) to Ala (generating mutant Aly^{5A}). The Aly^{5A} mutant should mimic Aly1 that has been permanently dephosphorylated by calcineurin. We also generated Aly1^{5E} to mimic Aly1 persistently phosphorylated at these same sites.

Phenotypic Effects of Calcineurin Regulation of Aly1—We showed previously that Aly1 overexpression confers an increase in resistance to rapamycin (Fig. 3*E*) (24). Although Aly1 and all the Aly1 phospho-mutants tested elevated resistance to rapamycin (Fig. 4*C*), we noted that cells expressing the Aly1 variants capable of being dephosphorylated by calcineurin (Aly1) or that mimic the dephosphorylated state (Aly1^{5A}) grew slightly better on rapamycin than cells expressing Aly1 variants that cannot be dephosphorylated by calcineurin (Aly1$^{\Delta PILKIN}$) or that mimic the persistently phosphorylated state (Aly1^{5E}) (Fig. 4*C*). This modest difference in phenotype was not due to differences in protein level as all of these GST fusions were expressed equivalently to wild-type Aly1 (Figs. 3*C*, 4*D*, and 7*A*) and behaved very similarly to wild-type Aly1 in other assays (Fig. 5, *A* and *E*, and data not shown).

In response to activation or inhibition of calcineurin activity, the electrophoretic migrations of Aly1^{5A} and Aly1^{5E} were indistinguishable from that of wild-type Aly1 (Fig. 4*D*), suggesting that additional calcineurin-regulated phospho-sites exist in Aly1 that were not pinpointed by our MS analyses (Fig. 4, *A* and *B*). However, further phenotypic characterization of Aly1^{5A} and Aly1^{5E} indicated (see last section under "Results") that the sites altered in these mutants are functionally important (Figs. 4*C* and 6, *B*–*G*).

Regulation by Calcineurin Is Not Required for Aly1-mediated Gap1 Trafficking—Phosphorylation of α-arrestins regulates arrestin-mediated trafficking of nutrient permeases (17, 24, 34, 35). Therefore, we examined whether dephosphorylation of Aly1 by calcineurin modulates either of the two trafficking functions described for Aly1 to date as follows: 1) regulation of Gap1 (general amino acid permease) intracellular sorting and 2) regulation of Dip5 (aspartic/glutamic acid permease) endocytosis (18, 24).

When nitrogen is limiting, Gap1 mediates entry of a wide range of amino acids, including proline (70). Uptake of two amino acid analogs, AzC, a toxic proline mimetic, and citrulline, an arginine mimetic taken up exclusively through Gap1, serve as readouts for Gap1 activity at the plasma membrane (55, 70). We showed previously that overexpression of either Aly1 or Aly2 results in hypersensitivity to AzC and an increase in the rate of citrulline uptake (24). Increased Gap1 activity at the cell surface is due to increased Gap1 retrieval from endosomes (likely via an endosome-to-Golgi route); impeding Gap1 trafficking to the vacuole (a degradative organelle) increases Gap1 levels in the cell and leads, ultimately, to an increased level of Gap1 at the plasma membrane (24). Thus, we tested whether the phosphorylation status of Aly1 influences Gap1 trafficking. We found that overexpression of Aly1, Aly1$^{\Delta PILKIN}$, Aly1^{5A}, or Aly1^{5E} each conferred an equivalent increase in sensitivity to AzC (Fig. 5*A*) and Gap1 protein levels (Fig. 5*C*). In addition, overexpression of either Aly1 or Aly1$^{\Delta PILKIN}$ caused a similar increase in the rate of citrulline uptake (Fig. 5*D*). To ensure that overexpression of these *ALY1* alleles was not masking subtle phenotypic differences between them, we examined the ability of Aly1 phospho-mutants expressed from low copy plasmids to complement the *aly1*Δ *aly2*Δ AzC resistance phenotype, and we found that all alleles restored AzC sensitivity equally (Fig. 5*B*).

Our earlier studies demonstrated that Aly2, but not Aly1, requires a number of factors to promote Gap1 recycling, including the following: Npr1, a nitrogen-regulated protein kinase that promotes Gap1 trafficking to the plasma membrane (35–37); Lst4, a factor known to stimulate nutrient-dependent recycling of Gap1 (22, 55), and AP-1, an adaptor complex that recruits clathrin to endosome-derived vesicles trafficking to the Golgi (24, 71, 72). Deletion of any of these factors cripples Aly2-stimulated Gap1 recycling and may thereby create a sensitized assay to detect subtle defects in Aly1-mediated Gap1 trafficking that might arise from loss of calcineurin regulation (24). By every metric employed (rate of citrulline uptake, growth using citrulline as sole nitrogen source, and sensitivity to AzC), overexpression of Aly1, Aly1$^{\Delta PILKIN}$, Aly1^{5A}, and Aly1^{5E} caused similar increases in Gap1 activity at the plasma membrane irrespective of the genetic background used (*npr1*Δ, *lst4*Δ, *apl2*Δ) (Fig. 5, *E* and *F*, and data not shown). Together, these findings indicate that dephosphorylation of Aly1 by calcineurin does not regulate Aly1-mediated Gap1 recycling.

Dephosphorylation of Aly1 by Calcineurin Is Required for Aly1-mediated Endocytosis of Dip5—A previous study by another group demonstrated that Aly2 promotes endocytosis

A Aly1 peptide coverage in MS analysis

MLQFNTENDTVAPVFPMEQDINAAPDAVPLVQTTTLQVFV**KLAEPIVFLKGFETNGLSEI**
APSILRGSLIV**RVLKPNK**L**KSISITFK**GIS**RTEWPEGIPPKR**EEFSDVETVVNHTWPFYQ
ADDGMNSFTLEHHSSNNSSN**RPSMSDEDYLLEKSGASVYIPPTAEPPKDNSNLSLDAYER**
NSLSSDNLSNKPVSSDVSHDDSKLLAIQKTPLPSSSRRRGSVPANFHGNSLSPHTFISDLF
T**KTFSNSGATPSPEQEDNYLTPSK**DS**KEVFIFRPGDYIYTFEQPISQSYPESIKANFGSV**
EYKLSIDIERFGAF**KSTIHTQLPIK**VV**RLPSDGSVEETEAIAISK**DW**KDLLHYDVVIFSK**
EIVLNAFLPIDFHFAPLDKVTLHRI**RIYLTESMEYTCNSNGNHEK**ARRLEPTK**KFLLAEH**
NGPKLPHIPAGSNPLKA**KNRGNILLDEKSGDLVNKDFQFEVFVPSKFTNSIR**LHPDTNYD
KIKAHHWIKICLRLSKKYGDNRKHFEISIDSPIHILNQLCSHANTLLPSYESHFQYCDED
GNFAPAADQQNYASHHDSNIFFP**KEVLSSPVLSPNVQK**MNI**RIPSDLPVVR**NRAESVKKS
KSDNTSK**KNDQSSNVFASKQLVANIYKPNQIPR**EL**TSPQALPLS**PITSPILNYQPLSNSP
PPDFDFDLA**KRGAADSHAIPVDPPSYFDVLKADGIELPYYDTSSSK**IPELKLNKSRETLA
SIEEDSFNGWSQIDDLSDEDDNDGDIASGFNF**KLSTSAPSENVNSHTPILQSLNMSLDGR**
KKNRASLHATSVLPSTIRQNNQHFNDINQMLGSSDEDAFPKSQSLNFNKKLPILKIN**DNV**
IQSNSNSNNRVDNPEDTVDSSVDITAFYDPRMSSDSKFDWEVSKNHVDPAAYSVNVASEN
RVLDDFKKAFREKRK*

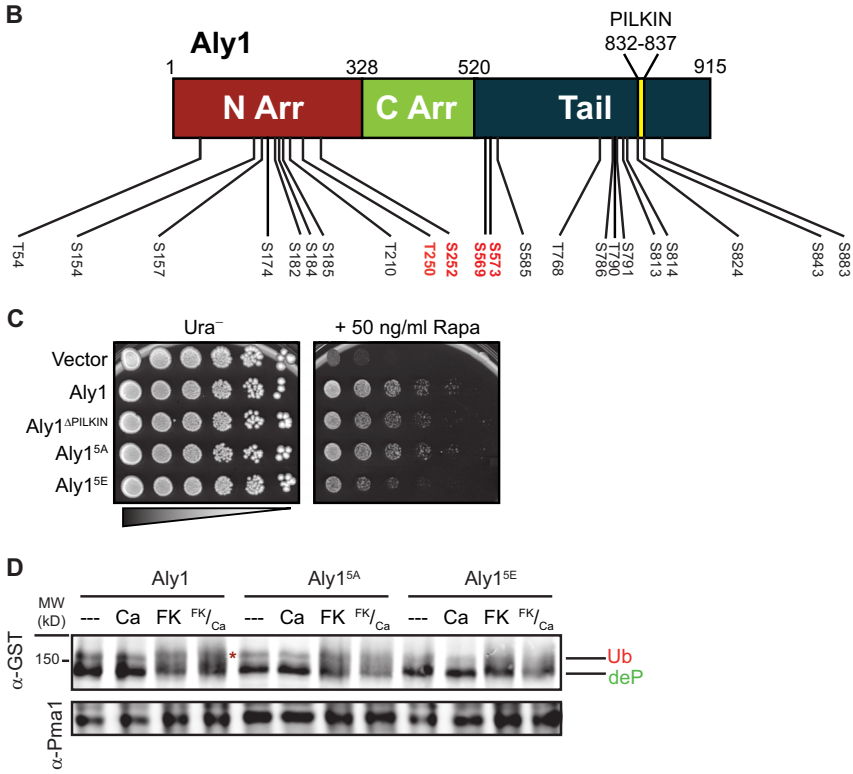

FIGURE 4. **Identification of a subset of Aly1 phospho-sites regulated by calcineurin.** *A,* map of Aly1 peptides sequences identified in the MS analysis. The *single letter code* for amino acids encoding Aly1 is shown with regions of the protein for which peptides were identified in each of the four MS analyses performed shown in *boldface green type*. The PILKIN calcineurin-docking motif is shown in *red*; no peptides containing the PILKIN sequence were identified in Aly1$^{\Delta PILKIN}$ samples. The predicted, putative 14-3-3-binding motifs in Aly1 are *underlined* (based on Scansite for Aly1 using a medium stringency assessment). *B,* schematic of the Aly1 protein with the N-terminal arrestin-fold domain (*N-Arr*; *red*), C-terminal arrestin-fold domain (*C-Arr*; *green*), C-terminal unstructured tail (*Tail*; *blue*) and approximate amino acid positions for domain boundaries (*numbers* along the top) shown (domains predicted using Phyre (82, 83)). The calcineurin docking-site (P*X*I*X*IT motif) is indicated in *yellow*. Positions of phospho-sites identified using MS analysis of Aly1 or Aly1$^{\Delta PILKIN}$ are shown as lines below the protein with the *single letter code* and sequence position provided for the amino acid. Sites regulated by calcineurin are indicated in *boldface red type*. *C,* growth of serial dilutions of BY4741 cells containing pRS426 (vector), pRS426-Aly1, pRS426-Aly1$^{\Delta PILKIN}$, pRS426-Aly1^{5A}, or pRS426-Aly1^{5E} on SC medium lacking uracil (Ura$^-$ control medium) or SC-Ura$^-$ with rapamycin (*Rapa*). *D,* WCE from BJ5459 cells expressing GST-Aly1, GST-Aly1^{5A} or GST-Aly1^{5E} were treated with nothing (−), 200 mM calcium chloride (*Ca*), 2 μg/ml FK506, or a combination of FK506 followed by Ca ($^{FK}/_{Ca}$) were generated by TCA extraction, resolved on 4% acrylamide gels, and assessed by immunoblotting. A *red asterisk* (*within the blot*) and line denoted with *Ub* (adjacent to blot) are used to help identify the ubiquitinylated species of Aly1.

of Dip5 in response to excess amounts of the amino acids transported by this permease (aspartic acid or glutamic acid), but it did not address directly whether Aly1 may also play a role in this process (18). Therefore, we tested whether regulation of Aly1 by calcineurin might alter its ability to stimulate Dip5 trafficking to the vacuole. We found that the absence of either Aly1 or Aly2 caused a detectable increase in the steady-state level of Dip5, and an even more pronounced increase was observed in cells lacking both Aly1 and Aly2 (Fig. 6*A*), as was observed previously (18). This is consistent with the idea that each of these

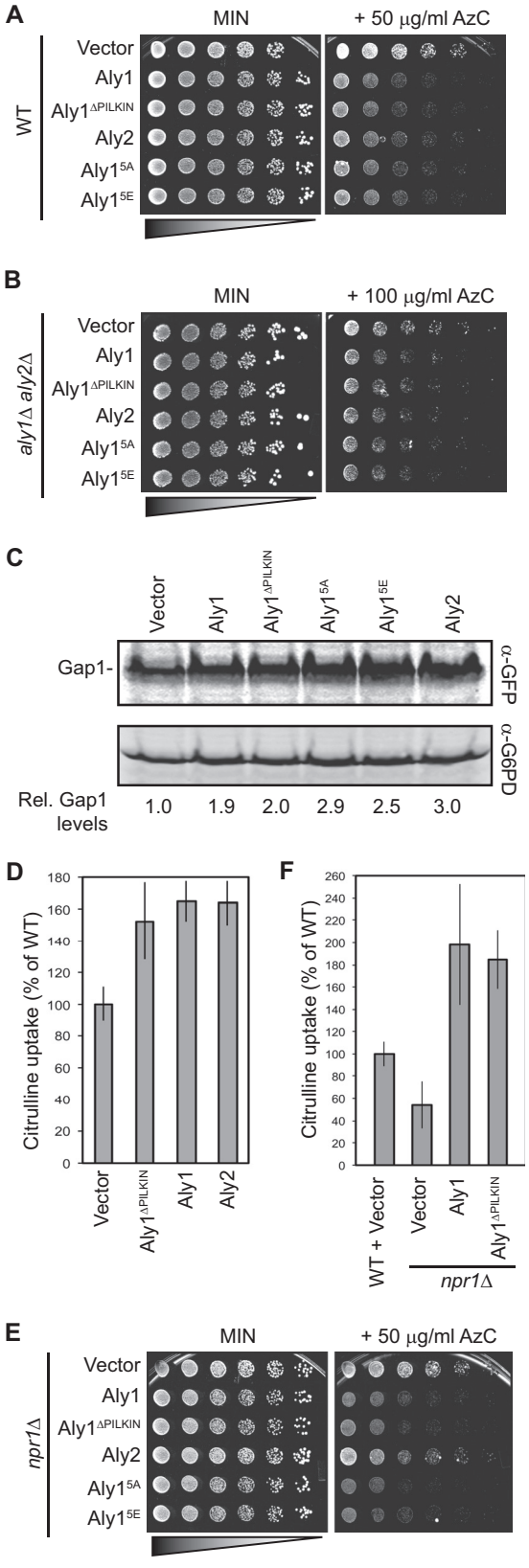

FIGURE 5. **CN regulation is not required for Aly1-mediated Gap1 recycling.** *A*, growth of serial dilutions of BY4741 cells containing pRS426 (*vector*), pRS426-Aly1, pRS426-Aly1$^{\Delta PILKIN}$, pRS426-Aly2, pRS426-Aly1^{5A}, or pRS426-Aly1^{5E} on MIN 0.5% $(NH_4)_2SO_4$ ± AzC. *B*, growth of serial dilutions of *aly1*Δ *aly2*Δ (D2–6A) cells containing pRS315 (*vector*), pRS315-Aly1, pRS315-Aly1$^{\Delta PILKIN}$, pRS315-Aly2, pRS315-Aly1^{5A}, or pRS315-Aly1^{5E} on MIN 0.5% $(NH_4)_2SO_4$ ± AzC. *C*, BY4743 cells containing pRS426 (vector, pRS426-Aly1 or pRS426-Aly1$^{\Delta PILKIN}$, pRS426-Aly1^{5A}, pRS426-Aly1^{5E}, or pRS426-Aly2) and pCKB230 (Gap1-GFP) were grown in MIN 0.5% $(NH_4)_2SO_4$. WCEs were resolved using SDS-PAGE, and Gap1 levels were assessed by immunoblotting. Gap1 levels relative to the vector control extract are presented *below* the immunoblot. *D* and *F*, prototrophic BY4741 (WT) or *npr1*Δ cells with pCK283 and pRS426, pRS426-Aly1, pRS426-Aly1$^{\Delta PILKIN}$, or pRS426-Aly2 were assayed for [^{14}C]citrulline uptake. The mean uptake rate for seven replicates (in *C*) or three replicates (in *E*) is shown as a percentage relative to the WT containing vector, and *error bars* represent ± S.D. *E*, growth of serial dilutions of *npr1*Δ cells with pRS425, pRS425-Aly1, pRS425-Aly1$^{\Delta PILKIN}$, pRS425-Aly2, pRS425-Aly1^{5A}, or pRS425-Aly1^{5E} on MIN 0.5% $(NH_4)_2SO_4$ ± AzC.

α-arrestins contributes to the endocytosis of Dip5. Therefore, as an independent means to assess the impact of Aly2 and Aly1 variants on Dip5 activity and trafficking, all subsequent analyses were performed in an *aly1*Δ *aly2*Δ background containing either a vector control or a low copy plasmid expressing the *ALY* allele of interest from its endogenous promoter. We measured Dip5 function at the cell surface by monitoring the rate of radiolabeled aspartic acid uptake and found that expression of Aly1, Aly1^{5A}, or Aly2 each significantly reduced the rate of aspartic acid uptake compared with the vector control (Fig. 6*B*), consistent with diminished Dip5 level and/or activity at the PM in these cells. By contrast, significantly higher Dip5 activity and/or levels were observed in cells expressing Aly1$^{\Delta PILKIN}$ or Aly1^{5E}, which maintains Aly1 in a hyperphosphorylated or phospho-mimetic state, compared with cells expressing either Aly1 or Aly1^{5A} (Fig. 6*B*), their dephosphorylated counterparts. These data support a role for Aly1 and Aly2 in basal turnover of Dip5 as the aspartic acid uptake assays are done over a very short time course (2 min) and so likely reflect differences in the steady-state levels of Dip5 operating at the plasma membrane.

To determine whether the observed effects were due to alterations in the level of Dip5 at the cell surface, steady-state localization of Dip5-GFP was examined in cells expressing various *ALY* alleles. For these experiments, cells containing *DIP5-GFP* integrated at its chromosomal locus were grown under conditions equivalent to those used for the aspartic acid uptake assays. Images (Fig. 6*C*) were quantified, and reported differences in Dip5-GFP fluorescence intensity were assessed statistically, both as the pixel count at the PM (Fig. 6*D*) and as the ratio of the pixel count at the PM to that in the vacuole of the same cell (Fig. 6*E*; see also "Experimental Procedures"). Despite some cell-to-cell variation in these cell populations, these analyses showed that expression of Aly2 (as a positive control), as well as Aly1 and Aly1^{5A}, significantly reduced the amount of Dip5 at the PM and increased the amount of Dip5 in the vacuole, compared with the *aly1*Δ *aly2*Δ controls cells carrying the vector alone (Fig. 6, *C–E*). In marked contrast, expression of Aly1$^{\Delta PILKIN}$ or Aly1^{5E} in the *aly1*Δ *aly2*Δ cells neither reduced the amount of Dip5 at the PM nor increased the amount of Dip5 in the vacuole (Fig. 6, *C–E*). It should be noted, however, that due to background cytoplasmic fluorescence the PM-to-vacuolar ratios presented in Fig. 6*E* are lower than expected for the vector control (and likely for the Aly1$^{\Delta PILKIN}$ and Aly1^{5E} alleles as well) based on the micrographs presented in Fig. 6*C*. These findings are consistent with the interpretation that phosphorylation blocks the ability of Aly1 to stimulate Dip5 internalization because Aly1 (which can be dephosphorylated by CN) and the Aly1^{5A} variant (which mimics its dephosphorylated state)

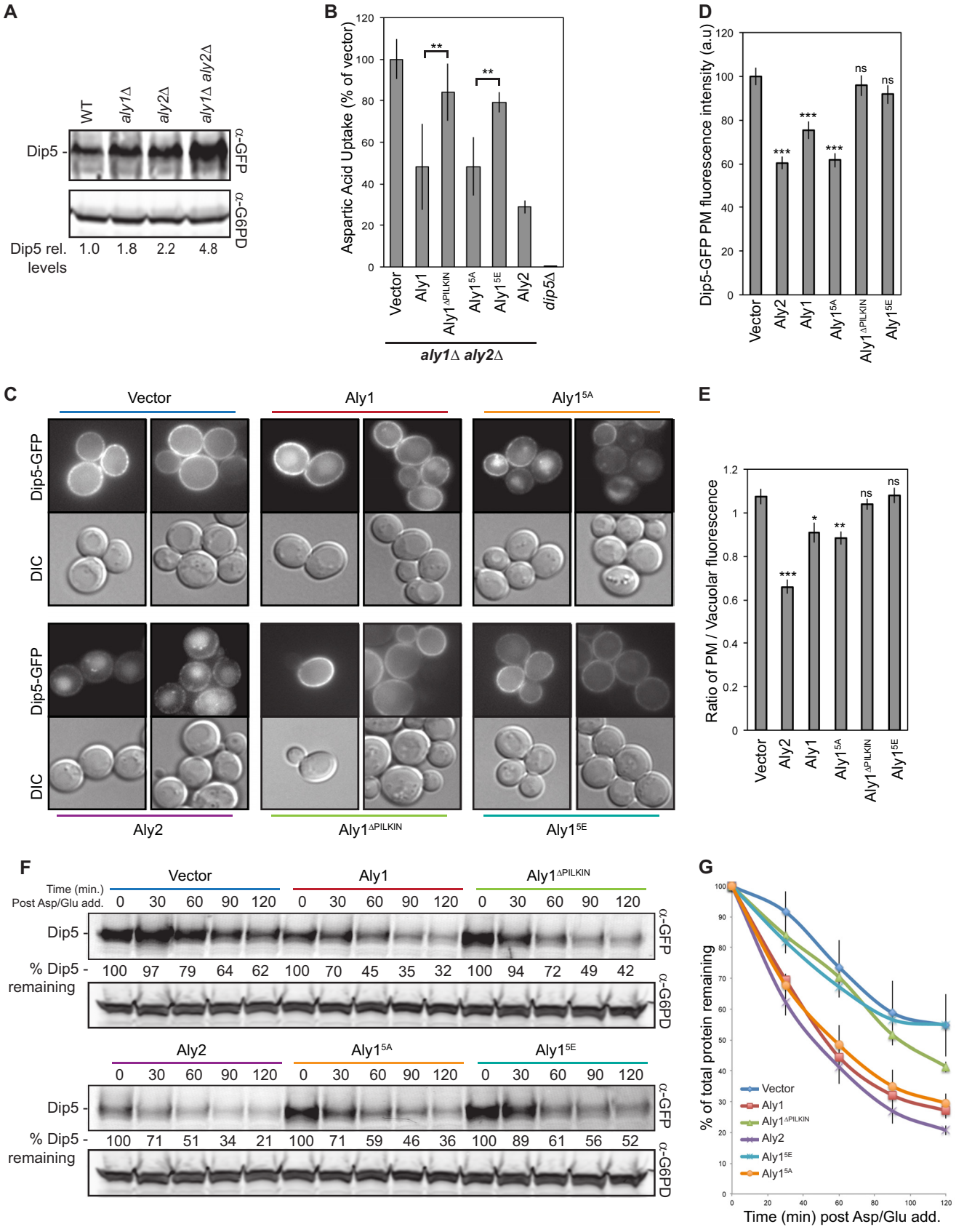

both promoted basal endocytosis of Dip5 in *aly1*Δ *aly2*Δ cells, whereas the Aly1$^{\Delta PILKIN}$ variant (which cannot bind CN) and the Aly1^{5E} phospho-mimetic mutant were unable to promote Dip5 endocytosis. Because these assays were done in the absence of substrate (no aspartic acid/glutamic acid ligand), the differences in Dip5 cell surface levels represent changes in the basal trafficking of Dip5 to the vacuole in the presence of these *ALY* alleles.

We also carried out kinetic analysis of Dip5 stability in response to exogenous aspartic acid and glutamic acid, which induces endocytosis of the Dip5 permease. After addition of aspartic acid and glutamic acid, degradation of Dip5-GFP was appreciably faster in cells containing Aly2, Aly1, or Aly1^{5A} than in cells expressing Aly1$^{\Delta PILKIN}$, Aly1^{5E}, or the control vector (Fig. 6, *F* and *G*). Moreover, even at the zero time point, cells expressing Aly2, Aly1, and Aly1^{5A} contained less Dip5 than cells containing Aly1$^{\Delta PILKIN}$, Aly1^{5E}, or a control vector (Fig. 6*F*), consistent with faster turnover of Dip5 when Aly2 or dephosphorylated Aly1 are present. Together, these data demonstrate that the phospho-mimetic Aly1^{5E} protein and Aly1$^{\Delta PILKIN}$, which cannot be dephosphorylated by calcineurin, fail to internalize and degrade Dip5 as effectively as wild-type Aly1 or the dephosphorylation-mimetic Aly1^{5A}. Thus, we conclude that dephosphorylation of Aly1 by calcineurin is required to promote Aly1-mediated trafficking of Dip5 to the vacuole.

Our data for Aly1 are consistent with recent findings that α-arrestins Rod1 and Bul1 must be dephosphorylated to promote nutrient-induced endocytosis of the Jen1 and Gap1 permeases, respectively. Dephosphorylation of Rod1 and Bul1 by unidentified phosphatases results in loss of binding to the yeast 14-3-3 proteins (Bmh1 and Bmh2), suggesting that it is their association with 14-3-3 proteins that may be responsible for inhibiting their endocytic function (17, 35). Because previous MS analyses revealed enrichment of Bmh1 and Bmh2 peptides in purified preparations of Aly1 and Aly2,[5] we examined whether calcineurin-mediated dephosphorylation of Aly1 alters its interaction with Bmh1 and Bmh2. We found that Bmh1 and Bmh2 copurified from yeast extracts with GST-Aly1 and GST-Aly2 but not with the GST control (Fig. 7), confirming our previous MS analyses. Although significantly higher levels of Bmh1 and Bmh2 copurified with Aly2 than with Aly1, the amount of Bmh1 and Bmh2 associated with Aly1, Aly1$^{\Delta PILKIN}$,

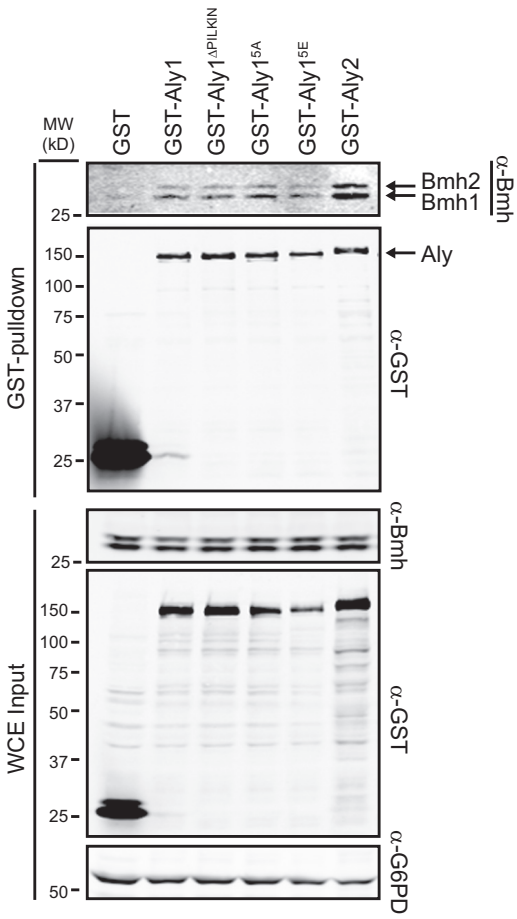

FIGURE 7. **CN-regulation of Aly1 does not alter Aly1-association with 14-3-3 proteins.** GST, GST-Aly1, GST-Aly1$^{\Delta PILKIN}$, GST-Aly1^{5A}, GST-Aly1^{5E}, or GST-Aly2 (expressed from pKK212-derived plasmids) were extracted and purified from BJ5459 cells using glutathione-Sepharose. Copurification of endogenous 14-3-3 proteins (Bmh1 is lower band and Bmh2 is upper band in doublet) was assessed by immunoblotting. 2% of the WCE used as input for pulldowns is shown.

FIGURE 6. **Calcineurin-mediated dephosphorylation of Aly1 is required for Aly1-dependent trafficking of Dip5 to the vacuole.** *A,* WCEs from BY4741, *aly1*Δ, *aly2*Δ, or *aly1*Δ *aly2*Δ cells containing a chromosomally integrated Dip5-GFP grown in MIN +0.5% $(NH_4)_2SO_4$ were resolved by SDS-PAGE, and Dip5 levels were assessed by immunoblotting. Dip5 levels were quantified and are presented relative to the wild-type extract *below* the immunoblot. *B,* cells lacking both *ALY1* and *ALY2* containing pRS315 (vector, pRS315-Aly1, pRS315-Aly1$^{\Delta PILKIN}$, pRS315-Aly1^{5A}, pRS315-Aly1^{5E}, or pRS315-Aly2) or cells lacking *DIP5* were assayed for [^{14}C]aspartic acid uptake. The mean uptake rate for a minimum of four replicates is shown as a percentage relative to *aly1*Δ *aly2*Δ with vector and *error bars* represent ± S.D. Unpaired Student's *t* tests were performed to assess the significance of these data; *** indicates a *p* value <0.0001. It should be noted that Aly1, Aly1^{5A}, and Aly2 were all significantly less than the vector control (*p* value <0.001) but were not significantly different from one another (*p* value >0.01). Similarly, Aly1$^{\Delta PILKIN}$ and Aly1^{5E} were not significantly different from one another (*p* value >0.01). *C,* Dip5-GFP in *aly1*Δ *aly2*Δ cells containing pRS315, -Aly2, -Aly1, -Aly1$^{\Delta PILKIN}$, -Aly1^{5A}, or -Aly1^{5E} was visualized by fluorescence microscopy, and two panels of representative cell images are presented for each. Aly2, Aly1, and the dephosphorylation mimetic (Aly1^{5A}) restore endocytosis of Dip5, as evidenced by vacuolar fluorescence in >46% of cells, although cells containing vector or mutants of that mimic the phosphorylated form of Aly1 have predominantly PM-localized Dip5 (<27% of cells displayed dim vacuolar fluorescence). *D,* plasma membrane fluorescence intensities for Dip5-GFP (as shown in *C*) were normalized to background and quantified for >140 cells per strain (see "Experimental Procedures"). The mean plasma membrane intensity is plotted ± S.E. (in arbitrary units). A one-way ANOVA with Tukey's post hoc comparison was used to assess the statistical significance of fluorescence differences compared with the vector control (***, *p* value <0.0001; *ns,* not significant *p* value >0.01). *E,* ratio of plasma membrane fluorescence to vacuolar fluorescence for Dip5-GFP (as shown in *C*) was measured for a minimum of 40 cells per condition (see "Experimental Procedures"). A one-way ANOVA with Tukey's post hoc comparison was used to assess the statistical significance for each of these ratios compared with the pRS315 vector control (***, *p* value <0.0001; **, *p* value <0.001; *, *p* value <0.01, and *ns* = not significant *p* value >0.01). *F, aly1*Δ *aly2*Δ cells containing pRS315, -Aly2, -Aly1, -Aly1$^{\Delta PILKIN}$, -Aly1^{5A}, or -Aly1^{5E} and a chromosomally integrated Dip5-GFP were grown in MIN +0.5% $(NH_4)_2SO_4$ medium, and 200 μg/ml aspartic acid and glutamic acid were added to trigger internalization and degradation of Dip5. Cells were harvested at the times indicated post-Asp/Glu addition; WCEs were prepared using TCA extraction and analyzed by SDS-PAGE and immunoblotting. Data representing one of the three replicate experiments performed are presented with the quantification for the percentage of Dip5 remaining in each lane relative to the $t = 0$ point and normalized for alterations in the G6PD loading control is indicated. *G,* Dip5-GFP band intensities from three replicate experiments (representative panel in *F*) were measured, normalized to the G6PD loading control, and the mean percentage of Dip5 remaining post Asp/Glu addition ± S.E. is plotted. DIC, differential interference contrast.

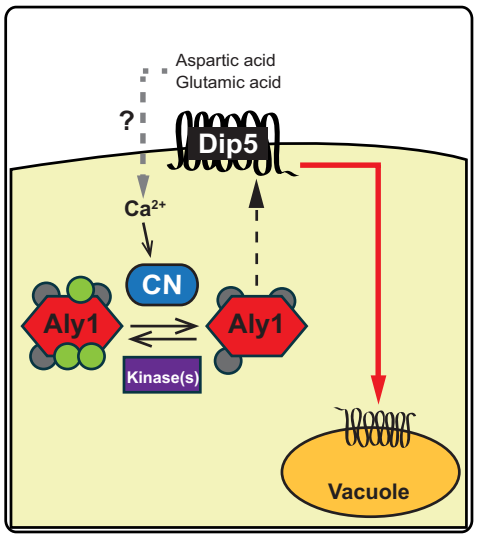

FIGURE 8. **Model for phospho-regulation of α-arrestin-mediated trafficking.** Unidentified kinases (*purple rectangle*) maintain Aly1 (*red hexagon*) in its fully phosphorylated state (phosphosites represented as *gray* and *green circles*), which is unable to stimulate internalization of the aspartic acid/glutamic acid transporter Dip5. When calcineurin (*CN*; *blue oval*) is activated by calcium, as may occur in response to excess aspartic acid/glutamic acid (indicated *gray dashed line*), it dephosphorylates Aly1, and this dephosphorylation at specific sites (removal of CN-regulated phosphosites; loss of *green circles*) is required for optimal Aly1-mediated endocytosis of Dip5. Dephosphorylated Aly1 promotes endocytosis and/or trafficking of Dip5 to the vacuole (indicated by *dashed black arrow* and trafficking route denoted by *red line*).

Aly1^{5A}, or Aly1^{5E} was not detectably different (Fig. 7). These findings suggest that phosphorylation of Aly1 at the CN-sensitive sites delineated in this study is not the major determinant of the association with Bmh1 and Bmh2. Indeed, there are two sites in Aly1 that fit the predicted 14-3-3-binding sites consensus, each of which lies in peptides not recovered in our MS analyses and neither of which map to any calcineurin-regulated phospho-site identified here (Fig. 4*A*). Thus, although dephosphorylation of other α-arrestins may serve as a regulatory mechanism to release these adaptors from the grasp of 14-3-3 proteins, and thereby promote α-arrestin-mediated endocytosis of permeases, that does not appear to be the underlying mechanism by which CN-mediated dephosphorylation stimulates the trafficking function of Aly1.

DISCUSSION

Phospho-regulation of Aly1-mediated Trafficking—We show here that α-arrestin Aly1 interacts with calcineurin through a C-terminal docking motif and identified up to five possible CN-targeted phospho-sites in Aly1. Furthermore, by monitoring the amino acid permease Dip5 as its cargo, we demonstrated that Aly1 must be dephosphorylated by calcineurin to mediate Dip5 trafficking to the vacuole (Fig. 8). This study is the first to identify a phosphatase that directly regulates α-arrestin function. Although phospho-sites have been identified for various α-arrestins in global proteomic screens (68, 69), aside from our work on Aly1, a comprehensive phospho-map exists for only one other α-arrestin, namely Ldb19/Art1 (34). Given that only a handful of the 22 phospho-residues detected in Aly1 appear to be regulated by calcineurin (and there appear to be additional calcineurin-regulated sites in Aly1 not identified in our study), Aly1 action may be under the control of multiple protein kinases and phosphatases. Indeed, other α-arrestins are highly modified, many with >10 phospho-sites identified to date (68, 69), underscoring the potential complexity of their regulation.

Both Aly1 and the related Aly2 promote retrieval of the general amino acid permease Gap1 from endosomes, and Npr1-dependent phosphorylation of Aly2 is needed for its function in this Gap1 recycling (24). We show here that dephosphorylation of Aly1 by calcineurin is not required for such Gap1 recycling, suggesting that different subsets of phospho-sites may regulate distinct α-arrestin trafficking functions. It was demonstrated that Aly2 is necessary for efficient endocytosis of the Dip5 transporter (18), but whether Aly1 might function semi-redundantly in this process was never directly tested. We show here that Aly1, when dephosphorylated by calcineurin, does stimulate Dip5 internalization and turnover, providing evidence that Aly1, like other α-arrestins, mediates the endocytosis of nutrient transporters.

Thus, our results indicate that Aly1 action is under control of a phosphorylation-dephosphorylation switch; calcineurin-mediated dephosphorylation stimulates Aly1 function in trafficking at least one membrane permease to the vacuole (Fig. 8), and phosphorylation, by an as yet unidentified protein kinase, inhibits it. Because excess aspartate or glutamate stimulates Dip5 internalization, and Aly1 can only mediate Dip5 down-regulation when dephosphorylated by calcineurin, influx of these acidic amino acids may stimulate calcineurin-dependent signaling through unknown mechanisms. In turn, dephosphorylated Aly1 promotes Dip5 endocytosis to the vacuole (Fig. 8), perhaps to prevent the cytotoxicity that an excess of these amino acids can cause (73). Indeed, in mammalian cells, amino acid overload increases the level of Ca^{2+}-calmodulin (74), a requirement for calcineurin activation.

Arrestin Dephosphorylation Is a Conserved Mechanism That Promotes Arrestin-mediated Endocytosis—Our data and other recent findings suggest a general model for phospho-regulation of α-arrestins (Fig. 8) (75). As shown here for Aly1/Art6, phosphorylation of Rod1/Art4 (17), Ldb19/Art1 (34), and two newly recognized α-arrestins Bul1 and Bul2 (35) blocks their ability to mediate endocytosis of specific nutrient permeases. In cells grown on lactate, the protein kinase Snf1 phosphorylates Rod1 to retain the lactic acid permease Jen1 at the plasma membrane; however, upon glucose addition, which inactivates Snf1, endocytosis of Jen1 ensues (17). Rod1 dephosphorylation appears to be PP1-dependent, but direct dephosphorylation of Rod1 by PP1 has not been demonstrated. Moreover, because PP1 action (Glc7-Reg1 complex) is necessary for inactivation of Snf1, the lack of apparent Rod1 dephosphorylation in *reg1*Δ cells may arise indirectly from lack of Snf1 down-regulation. For Ldb19, phosphorylation by the protein kinase Npr1 impairs Ldb19-mediated endocytosis of the arginine permease Can1, whereas the dephosphorylated protein associates with the plasma membrane and promotes Can1 endocytosis (34). However, the phosphatase responsible for Ldb19 dephosphorylation is not known. For Bul1 and Bul2, phosphorylation by Npr1, which is activated on poor nitrogen sources (*e.g.* proline), inhibits Bul-mediated endocytosis of Gap1. When NH_4^+ is the nitrogen source, Npr1 is inactive, and the Bul proteins are dephosphorylated in a man-

ner that depends on the phosphatase Sit4, promoting Gap1 internalization (35). However, direct dephosphorylation of Bul1 or Bul2 by Sit4 has not been demonstrated.

Thus, in the case of Aly1 and three other yeast α-arrestins, phosphorylation blocks and dephosphorylation promotes their endocytic function. Indeed, this phospho-inhibition of α-arrestin-mediated endocytosis is conserved in mammals. For example, phosphorylation of α-arrestin TNXIP by AMPK results in reduced stability of this α-arrestin, diminishing endocytic turnover of the GLUT1 glucose transporter regulated by TXNIP (32). However, the evidence to date indicates that phosphorylation can modulate α-arrestin function through distinct mechanisms. First, in the case of yeast Rod1, dephosphorylation of the α-arrestin promotes its endocytic function and is required for its ubiquitinylation (17). In contrast, dephosphorylation does not seem to regulate the ubiquitinylation of either Aly1, as we have shown here, or Bul1 (35). Similarly, under conditions that do not promote Ldb19-mediated internalization of Can1, this α-arrestin is ubiquitinylated, further supporting the idea that α-arrestin ubiquitinylation and its endocytic function need not be coupled (20, 34). Second, phosphorylation reportedly regulates the interactions of Rod1, Bul1, and Bul2 with cytoplasmic 14-3-3 proteins, resulting in sequestration of the α-arrestin (or the α-arrestin·Rsp5 complex) in the cytosol, and thereby inhibiting α-arrestin activity at and/or recruitment to the plasma membrane (17, 32, 35). Other α-arrestins are among the 271 proteins demonstrated to associate with Bmh1 and Bmh2 in a phosphorylation-dependent manner (76); therefore, interaction with 14-3-3 proteins may broadly regulate α-arrestin function. However, neither of these mechanisms is adequate to explain phospho-regulation of Aly1, because we demonstrated here that the calcineurin-dependent dephosphorylation of Aly1 does not alter its ubiquitinylation, stability, or interaction with either Rsp5 or 14-3-3 proteins. Dephosphorylation of mammalian β-arrestins is required for their association with clathrin and AP-2 and subsequent stimulation of endocytosis (6, 10). Both Aly1 and Aly2 have been shown to interact with clathrin adaptors (24); therefore, phosphorylation might similarly regulate the endocytic function of Aly1 by altering its interaction with these components of the trafficking machinery.

Conserved Interaction of Calcineurin with α-Arrestins and Its Implications—A *Caenorhabditis elegans* α-arrestin, CNP-1/ArrD-17, interacts with the catalytic subunit of calcineurin and is a calcineurin substrate *in vitro* (57). Although no calcineurin-docking site was identified in the nematode protein, we note that CNP-1/ArrD-17 contains near its C terminus a variant P*X*L*X*IT motif (PIVIGS) that is conserved in its mammalian α-arrestin relatives ARRDC2–4 and TNXIP (as PLVIGS or PLVIGT). Interestingly, calcineurin regulation of ArrD-17 in *C. elegans* also impacts response to starvation, although a link between specific α-arrestins and trafficking of any nutrient transporter has not yet been established.

To our knowledge, our work is the first demonstration that calcineurin dephosphorylates an α-arrestin to regulate the trafficking function of this class of adaptor proteins. However, calcineurin action influences membrane protein trafficking in other ways. For example, heat stress-induced calcineurin-mediated dephosphorylation of the TORC2- and eisosome-associated components Slm1 and Slm2 stimulates internalization of the uracil permease Fur4 (45, 62, 77). Studies of synaptic vesicle retrieval in mammalian cells indicate that calcineurin dephosphorylates a suite of endocytic regulators, including amphiphysins, synaptojanin, epsins, and dynamin (78, 79). Calcineurin activation also stimulates receptor-mediated endocytosis of AMPA and transferrin (80, 81). Collectively, and combined with our demonstration here that calcineurin regulates α-arrestin-mediated trafficking to the vacuole in yeast, it is clear that calcineurin has an important physiological function as a global regulator of membrane protein trafficking.

Acknowledgments—We gratefully acknowledge Marko Kaksonen (EMBL, Heidelberg, Germany) for providing the MKY yeast strains prior to their publication; Sandra Lemmon (University of Miami, FL) for providing the anti-Bmh antibody; and colleagues Alexander Sorkin, Jeffrey Brodsky, and Adam Kwiatkowski (University of Pittsburgh) for use of reagents and equipment. We thank Catherine Baty and Jenny Karlsson at the Center for Biological Imaging for assistance with cell imaging. We thank Lori Kohlstaedt (supported by National Institutes of Health Grant S10 RR025622-01) and the Vincent J. Coates Proteomics/Mass Spectrometry Laboratory at the University of California, Berkeley, for generating and analyzing the MS data.

REFERENCES

1. Sorkin, A., and von Zastrow, M. (2009) Endocytosis and signalling: intertwining molecular networks. *Nat. Rev. Mol. Cell Biol.* **10,** 609–622
2. DeWire, S. M., Ahn, S., Lefkowitz, R. J., and Shenoy, S. K. (2007) β-Arrestins and cell signaling. *Annu. Rev. Physiol.* **69,** 483–510
3. Moore, C. A., Milano, S. K., and Benovic, J. L. (2007) Regulation of receptor trafficking by GRKs and arrestins. *Annu. Rev. Physiol.* **69,** 451–482
4. Hong, M. H., Xu, C., Wang, Y. J., Ji, J. L., Tao, Y. M., Xu, X. J., Chen, J., Xie, X., Chi, Z. Q., and Liu, J. G. (2009) Role of Src in ligand-specific regulation of δ-opioid receptor desensitization and internalization. *J. Neurochem.* **108,** 102–114
5. Kim, Y. M., Barak, L. S., Caron, M. G., and Benovic, J. L. (2002) Regulation of arrestin-3 phosphorylation by casein kinase II. *J. Biol. Chem.* **277,** 16837–16846
6. Lin, F. T., Chen, W., Shenoy, S., Cong, M., Exum, S. T., and Lefkowitz, R. J. (2002) Phosphorylation of β-arrestin2 regulates its function in internalization of β_2-adrenergic receptors. *Biochemistry* **41,** 10692–10699
7. Lin, F. T., Daaka, Y., and Lefkowitz, R. J. (1998) β-Arrestins regulate mitogenic signaling and clathrin-mediated endocytosis of the insulin-like growth factor I receptor. *J. Biol. Chem.* **273,** 31640–31643
8. Lin, F. T., Krueger, K. M., Kendall, H. E., Daaka, Y., Fredericks, Z. L., Pitcher, J. A., and Lefkowitz, R. J. (1997) Clathrin-mediated endocytosis of the β-adrenergic receptor is regulated by phosphorylation/dephosphorylation of β-arrestin1. *J. Biol. Chem.* **272,** 31051–31057
9. Luttrell, L. M., and Lefkowitz, R. J. (2002) The role of β-arrestins in the termination and transduction of G-protein-coupled receptor signals. *J. Cell Sci.* **115,** 455–465
10. Marion, S., Fralish, G. B., Laporte, S., Caron, M. G., and Barak, L. S. (2007) N-terminal tyrosine modulation of the endocytic adaptor function of the β-arrestins. *J. Biol. Chem.* **282,** 18937–18944
11. Alvarez, C. E. (2008) On the origins of arrestin and rhodopsin. *BMC Evol. Biol.* **8,** 222
12. Nikko, E., and Pelham, H. R. (2009) Arrestin-mediated endocytosis of yeast plasma membrane transporters. *Traffic* **10,** 1856–1867
13. Novoselova, T. V., Zahira, K., Rose, R. S., and Sullivan, J. A. (2012) Bul proteins, a nonredundant, antagonistic family of ubiquitin ligase regulatory proteins. *Eukaryot. Cell* **11,** 463–470
14. Sonnhammer, E. L., Eddy, S. R., Birney, E., Bateman, A., and Durbin, R.

(1998) Pfam: multiple sequence alignments and HMM-profiles of protein domains. *Nucleic Acids Res.* **26,** 320–322
15. Léon, S., and Haguenauer-Tsapis, R. (2009) Ubiquitin ligase adaptors: regulators of ubiquitylation and endocytosis of plasma membrane proteins. *Exp. Cell Res.* **315,** 1574–1583
16. Rotin, D., and Kumar, S. (2009) Physiological functions of the HECT family of ubiquitin ligases. *Nat. Rev. Mol. Cell Biol.* **10,** 398–409
17. Becuwe, M., Vieira, N., Lara, D., Gomes-Rezende, J., Soares-Cunha, C., Casal, M., Haguenauer-Tsapis, R., Vincent, O., Paiva, S., and Léon, S. (2012) A molecular switch on an arrestin-like protein relays glucose signaling to transporter endocytosis. *J. Cell Biol.* **196,** 247–259
18. Hatakeyama, R., Kamiya, M., Takahara, T., and Maeda, T. (2010) Endocytosis of the aspartic acid/glutamic acid transporter Dip5 is triggered by substrate-dependent recruitment of the Rsp5 ubiquitin ligase via the arrestin-like protein Aly2. *Mol. Cell. Biol.* **30,** 5598–5607
19. Herrador, A., Herranz, S., Lara, D., and Vincent, O. (2010) Recruitment of the ESCRT machinery to a putative seven-transmembrane-domain receptor is mediated by an arrestin-related protein. *Mol. Cell. Biol.* **30,** 897–907
20. Lin, C. H., MacGurn, J. A., Chu, T., Stefan, C. J., and Emr, S. D. (2008) Arrestin-related ubiquitin-ligase adaptors regulate endocytosis and protein turnover at the cell surface. *Cell* **135,** 714–725
21. Nikko, E., Sullivan, J. A., and Pelham, H. R. (2008) Arrestin-like proteins mediate ubiquitination and endocytosis of the yeast metal transporter Smf1. *EMBO Rep.* **9,** 1216–1221
22. Helliwell, S. B., Losko, S., and Kaiser, C. A. (2001) Components of a ubiquitin ligase complex specify polyubiquitination and intracellular trafficking of the general amino acid permease. *J. Cell Biol.* **153,** 649–662
23. Lauwers, E., Jacob, C., and André, B. (2009) K63-linked ubiquitin chains as a specific signal for protein sorting into the multivesicular body pathway. *J. Cell Biol.* **185,** 493–502
24. O'Donnell, A. F., Apffel, A., Gardner, R. G., and Cyert, M. S. (2010) α-Arrestins Aly1 and Aly2 regulate intracellular trafficking in response to nutrient signaling. *Mol. Biol. Cell* **21,** 3552–3566
25. Soetens, O., De Craene, J. O., and Andre, B. (2001) Ubiquitin is required for sorting to the vacuole of the yeast general amino acid permease, Gap1. *J. Biol. Chem.* **276,** 43949–43957
26. Nabhan, J. F., Pan, H., and Lu, Q. (2010) Arrestin domain-containing protein 3 recruits the NEDD4 E3 ligase to mediate ubiquitination of the β2-adrenergic receptor. *EMBO Rep.* **11,** 605–611
27. Patwari, P., Chutkow, W. A., Cummings, K., Verstraeten, V. L., Lammerding, J., Schreiter, E. R., and Lee, R. T. (2009) Thioredoxin-independent regulation of metabolism by the α-arrestin proteins. *J. Biol. Chem.* **284,** 24996–25003
28. Patwari, P., Emilsson, V., Schadt, E. E., Chutkow, W. A., Lee, S., Marsili, A., Zhang, Y., Dobrin, R., Cohen, D. E., Larsen, P. R., Zavacki, A. M., Fong, L. G., Young, S. G., and Lee, R. T. (2011) The arrestin domain-containing 3 protein regulates body mass and energy expenditure. *Cell metabolism* **14,** 671–683
29. Vina-Vilaseca, A., Bender-Sigel, J., Sorkina, T., Closs, E. I., and Sorkin, A. (2011) Protein kinase C-dependent ubiquitination and clathrin-mediated endocytosis of the cationic amino acid transporter CAT-1. *J. Biol. Chem.* **286,** 8697–8706
30. Zhang, P., Wang, C., Gao, K., Wang, D., Mao, J., An, J., Xu, C., Wu, D., Yu, H., Liu, J. O., and Yu, L. (2010) The ubiquitin ligase itch regulates apoptosis by targeting thioredoxin-interacting protein for ubiquitin-dependent degradation. *J. Biol. Chem.* **285,** 8869–8879
31. Draheim, K. M., Chen, H. B., Tao, Q., Moore, N., Roche, M., and Lyle, S. (2010) ARRDC3 suppresses breast cancer progression by negatively regulating integrin β4. *Oncogene* **29,** 5032–5047
32. Wu, N., Zheng, B., Shaywitz, A., Dagon, Y., Tower, C., Bellinger, G., Shen, C. H., Wen, J., Asara, J., McGraw, T. E., Kahn, B. B., and Cantley, L. C. (2013) AMPK-dependent degradation of TXNIP upon energy stress leads to enhanced glucose uptake via GLUT1. *Mol. Cell* **49,** 1167–1175
33. Polo, S., and Di Fiore, P. P. (2008) Finding the right partner: science or ART? *Cell* **135,** 590–592
34. MacGurn, J. A., Hsu, P. C., Smolka, M. B., and Emr, S. D. (2011) TORC1 regulates endocytosis via Npr1-mediated phosphoinhibition of a ubiquitin ligase adaptor. *Cell* **147,** 1104–1117
35. Merhi, A., and André, B. (2012) Internal amino acids promote Gap1 permease ubiquitylation via TORC1/Npr1/14-3-3-dependent control of the Bul arrestin-like adaptors. *Mol. Cell. Biol.* **32,** 4510–4522
36. De Craene, J. O., Soetens, O., and Andre, B. (2001) The Npr1 kinase controls biosynthetic and endocytic sorting of the yeast Gap1 permease. *J. Biol. Chem.* **276,** 43939–43948
37. Schmidt, A., Beck, T., Koller, A., Kunz, J., and Hall, M. N. (1998) The TOR nutrient signalling pathway phosphorylates NPR1 and inhibits turnover of the tryptophan permease. *EMBO J.* **17,** 6924–6931
38. Aramburu, J., Heitman, J., and Crabtree, G. R. (2004) Calcineurin: a central controller of signalling in eukaryotes. *EMBO Rep.* **5,** 343–348
39. Li, H., Rao, A., and Hogan, P. G. (2011) Interaction of calcineurin with substrates and targeting proteins. *Trends Cell Biol.* **21,** 91–103
40. Cyert, M. S. (2003) Calcineurin signaling in *Saccharomyces cerevisiae*: how yeast go crazy in response to stress. *Biochem. Biophys. Res. Commun.* **311,** 1143–1150
41. Roy, J., and Cyert, M. S. (2009) Cracking the phosphatase code: docking interactions determine substrate specificity. *Sci. Signal.* **2,** re9
42. Yoshimoto, H., Saltsman, K., Gasch, A. P., Li, H. X., Ogawa, N., Botstein, D., Brown, P. O., and Cyert, M. S. (2002) Genome-wide analysis of gene expression regulated by the calcineurin/Crz1p signaling pathway in *Saccharomyces cerevisiae*. *J. Biol. Chem.* **277,** 31079–31088
43. Heath, V. L., Shaw, S. L., Roy, S., and Cyert, M. S. (2004) Hph1p and Hph2p, novel components of calcineurin-mediated stress responses in *Saccharomyces cerevisiae*. *Eukaryot. Cell* **3,** 695–704
44. Piña, F. J., O'Donnell, A. F., Pagant, S., Piao, H. L., Miller, J. P., Fields, S., Miller, E. A., and Cyert, M. S. (2011) Hph1 and Hph2 are novel components of the Sec63/Sec62 posttranslational translocation complex that aid in vacuolar proton ATPase biogenesis. *Eukaryot. Cell* **10,** 63–71
45. Bultynck, G., Heath, V. L., Majeed, A. P., Galan, J. M., Haguenauer-Tsapis, R., and Cyert, M. S. (2006) Slm1 and slm2 are novel substrates of the calcineurin phosphatase required for heat stress-induced endocytosis of the yeast uracil permease. *Mol. Cell. Biol.* **26,** 4729–4745
46. Johnston, G. C., Pringle, J. R., and Hartwell, L. H. (1977) Coordination of growth with cell division in the yeast *Saccharomyces cerevisiae*. *Exp. Cell Res.* **105,** 79–98
47. James, P., Halladay, J., and Craig, E. A. (1996) Genomic libraries and a host strain designed for highly efficient two-hybrid selection in yeast. *Genetics* **144,** 1425–1436
48. Ausubel, F. M., Brent, R., Kingston, R. E., Moore, D. D., Seidman, J. G., Smith, J. A., and Struhl, K. (1991) *Current Protocols in Molecular Biology*, pp. 13.7.1–13.7.10, John Wiley & Sons, Inc., New York
49. Sambrook, J., Fritsch, E. F., and Maniatis, T. (1989) *Molecular Cloning: A Laboratory Manual*, pp. 1.53–1.84; 6.3–6.17, Cold Spring Harbor Laboratory Press, NY
50. Sanger, F., Air, G. M., Barrell, B. G., Brown, N. L., Coulson, A. R., Fiddes, C. A., Hutchison, C. A., Slocombe, P. M., and Smith, M. (1977) Nucleotide sequence of bacteriophage ϕX174 DNA. *Nature* **265,** 687–695
51. Volland, C., Urban-Grimal, D., Géraud, G., and Haguenauer-Tsapis, R. (1994) Endocytosis and degradation of the yeast uracil permease under adverse conditions. *J. Biol. Chem.* **269,** 9833–9841
52. Laemmli, U. K. (1970) Cleavage of structural proteins during the assembly of the head of bacteriophage T4. *Nature* **227,** 680–685
53. Baum, P., Thorner, J., and Honig, L. (1978) Identification of tubulin from the yeast *Saccharomyces cerevisiae*. *Proc. Natl. Acad. Sci. U.S.A.* **75,** 4962–4966
54. Wolters, D. A., Washburn, M. P., and Yates, J. R., 3rd (2001) An automated multidimensional protein identification technology for shotgun proteomics. *Anal. Chem.* **73,** 5683–5690
55. Roberg, K. J., Bickel, S., Rowley, N., and Kaiser, C. A. (1997) Control of amino acid permease sorting in the late secretory pathway of *Saccharomyces cerevisiae* by SEC13, LST4, LST7, and LST8. *Genetics* **147,** 1569–1584
56. Rubio-Texeira, M., and Kaiser, C. A. (2006) Amino acids regulate retrieval of the yeast general amino acid permease from the vacuolar targeting pathway. *Mol. Biol. Cell* **17,** 3031–3050
57. Jee, C., Choi, T. W., Kalichamy, K., Yee, J. Z., Song, H. O., Ji, Y. J., Lee, J., Lee, J. I., L'Etoile, N. D., Ahnn, J., and Lee, S. K. (2012) CNP-1 (ARRD-17),

a novel substrate of calcineurin, is critical for modulation of egg-laying and locomotion in response to food and lysine sensation in *Caenorhabditis elegans*. *J. Mol. Biol.* **417,** 165–178
58. Uetz, P., Giot, L., Cagney, G., Mansfield, T. A., Judson, R. S., Knight, J. R., Lockshon, D., Narayan, V., Srinivasan, M., Pochart, P., Qureshi-Emili, A., Li, Y., Godwin, B., Conover, D., Kalbfleisch, T., Vijayadamodar, G., Yang, M., Johnston, M., Fields, S., and Rothberg, J. M. (2000) A comprehensive analysis of protein-protein interactions in *Saccharomyces cerevisiae*. *Nature* **403,** 623–627
59. Aramburu, J., Garcia-Cózar, F., Raghavan, A., Okamura, H., Rao, A., and Hogan, P. G. (1998) Selective inhibition of NFAT activation by a peptide spanning the calcineurin targeting site of NFAT. *Mol. Cell* **1,** 627–637
60. Boustany, L. M., and Cyert, M. S. (2002) Calcineurin-dependent regulation of Crz1p nuclear export requires Msn5p and a conserved calcineurin-docking site. *Genes Dev.* **16,** 608–619
61. Stathopoulos-Gerontides, A., Guo, J. J., and Cyert, M. S. (1999) Yeast calcineurin regulates nuclear localization of the Crz1p transcription factor through dephosphorylation. *Genes Dev.* **13,** 798–803
62. Tabuchi, M., Audhya, A., Parsons, A. B., Boone, C., and Emr, S. D. (2006) The phosphatidylinositol 4,5-biphosphate and TORC2-binding proteins Slm1 and Slm2 function in sphingolipid regulation. *Mol. Cell. Biol.* **26,** 5861–5875
63. Kafadar, K. A., Zhu, H., Snyder, M., and Cyert, M. S. (2003) Negative regulation of calcineurin signaling by Hrr25p, a yeast homolog of casein kinase I. *Genes Dev.* **17,** 2698–2708
64. Schwaninger, M., Blume, R., Oetjen, E., and Knepel, W. (1993) The immunosuppressive drugs cyclosporin A and FK506 inhibit calcineurin phosphatase activity and gene transcription mediated through the cAMP-responsive element in a nonimmune cell line. *Naunyn Schmiedebergs Arch. Pharmacol.* **348,** 541–545
65. Roy, J., Li, H., Hogan, P. G., and Cyert, M. S. (2007) A conserved docking site modulates substrate affinity for calcineurin, signaling output, and *in vivo* function. *Mol. Cell* **25,** 889–901
66. Gupta, R., Kus, B., Fladd, C., Wasmuth, J., Tonikian, R., Sidhu, S., Krogan, N. J., Parkinson, J., and Rotin, D. (2007) Ubiquitination screen using protein microarrays for comprehensive identification of Rsp5 substrates in yeast. *Mol. Syst. Biol.* **3,** 116
67. Zheng, X. F., Florentino, D., Chen, J., Crabtree, G. R., and Schreiber, S. L. (1995) TOR kinase domains are required for two distinct functions, only one of which is inhibited by rapamycin. *Cell* **82,** 121–130
68. Bodenmiller, B., Campbell, D., Gerrits, B., Lam, H., Jovanovic, M., Picotti, P., Schlapbach, R., and Aebersold, R. (2008) PhosphoPep–a database of protein phosphorylation sites in model organisms. *Nat. Biotechnol.* **26,** 1339–1340
69. Stark, C., Su, T. C., Breitkreutz, A., Lourenco, P., Dahabieh, M., Breitkreutz, B. J., Tyers, M., and Sadowski, I. (2010) PhosphoGRID: a database of experimentally verified *in vivo* protein phosphorylation sites from the budding yeast *Saccharomyces cerevisiae*. *Database* 2010, bap026
70. Grenson, M., Hou, C., and Crabeel, M. (1970) Multiplicity of the amino acid permeases in *Saccharomyces cerevisiae*. IV. Evidence for a general amino acid permease. *J. Bacteriol.* **103,** 770–777
71. Valdivia, R. H., Baggott, D., Chuang, J. S., and Schekman, R. W. (2002) The yeast clathrin adaptor protein complex 1 is required for the efficient retention of a subset of late Golgi membrane proteins. *Dev. Cell* **2,** 283–294
72. Waguri, S., Dewitte, F., Le Borgne, R., Rouillé, Y., Uchiyama, Y., Dubremetz, J. F., and Hoflack, B. (2003) Visualization of TGN to endosome trafficking through fluorescently labeled MPR and AP-1 in living cells. *Mol. Biol. Cell* **14,** 142–155
73. Risinger, A. L., Cain, N. E., Chen, E. J., and Kaiser, C. A. (2006) Activity-dependent reversible inactivation of the general amino acid permease. *Mol. Biol. Cell* **17,** 4411–4419
74. Gulati, P., Gaspers, L. D., Dann, S. G., Joaquin, M., Nobukuni, T., Natt, F., Kozma, S. C., Thomas, A. P., and Thomas, G. (2008) Amino acids activate mTOR complex 1 via Ca^{2+}/CaM signaling to hVps34. *Cell Metab.* **7,** 456–465
75. O'Donnell, A. F. (2012) The running of the Buls: control of permease trafficking by α-arrestins Bul1 and Bul2. *Mol. Cell. Biol.* **32,** 4506–4509
76. Kakiuchi, K., Yamauchi, Y., Taoka, M., Iwago, M., Fujita, T., Ito, T., Song, S. Y., Sakai, A., Isobe, T., and Ichimura, T. (2007) Proteomic analysis of *in vivo* 14-3-3 interactions in the yeast *Saccharomyces cerevisiae*. *Biochemistry* **46,** 7781–7792
77. Kamble, C., Jain, S., Murphy, E., and Kim, K. (2011) Requirements of Slm proteins for proper eisosome organization, endocytic trafficking and recycling in the yeast *Saccharomyces cerevisiae*. *J. Biosci.* **36,** 79–96
78. Cousin, M. A., and Robinson, P. J. (2001) The dephosphins: dephosphorylation by calcineurin triggers synaptic vesicle endocytosis. *Trends Neurosci.* **24,** 659–665
79. Xue, J., Graham, M. E., Novelle, A. E., Sue, N., Gray, N., McNiven, M. A., Smillie, K. J., Cousin, M. A., and Robinson, P. J. (2011) Calcineurin selectively docks with the dynamin Ixb splice variant to regulate activity-dependent bulk endocytosis. *J. Biol. Chem.* **286,** 30295–30303
80. Beattie, E. C., Carroll, R. C., Yu, X., Morishita, W., Yasuda, H., von Zastrow, M., and Malenka, R. C. (2000) Regulation of AMPA receptor endocytosis by a signaling mechanism shared with LTD. *Nat. Neurosci.* **3,** 1291–1300
81. Lai, M. M., Luo, H. R., Burnett, P. E., Hong, J. J., and Snyder, S. H. (2000) The calcineurin-binding protein cain is a negative regulator of synaptic vesicle endocytosis. *J. Biol. Chem.* **275,** 34017–34020
82. Bennett-Lovsey, R. M., Herbert, A. D., Sternberg, M. J., and Kelley, L. A. (2008) Exploring the extremes of sequence/structure space with ensemble fold recognition in the program Phyre. *Proteins* **70,** 611–625
83. Kelley, L. A., and Sternberg, M. J. (2009) Protein structure prediction on the Web: a case study using the Phyre server. *Nat. Protoc.* **4,** 363–371
84. Winzeler, E. A., Shoemaker, D. D., Astromoff, A., Liang, H., Anderson, K., Andre, B., Bangham, R., Benito, R., Boeke, J. D., Bussey, H., Chu, A. M., Connelly, C., Davis, K., Dietrich, F., Dow, S. W., El Bakkoury, M., Foury, F., Friend, S. H., Gentalen, E., Giaever, G., Hegemann, J. H., Jones, T., Laub, M., Liao, H., Liebundguth, N., Lockhart, D. J., Lucau-Danila, A., Lussier, M., M'Rabet, N., Menard, P., Mittmann, M., Pai, C., Rebischung, C., Revuelta, J. L., Riles, L., Roberts, C. J., Ross-MacDonald, P., Scherens, B., Snyder, M., Sookhai-Mahadeo, S., Storms, R. K., Véronneau, S., Voet, M., Volckaert, G., Ward, T. R., Wysocki, R., Yen, G. S., Yu, K., Zimmermann, K., Philippsen, P., Johnston, M., and Davis, R. W. (1999) Functional characterization of the *S. cerevisiae* genome by gene deletion and parallel analysis. *Science* **285,** 901–906
85. Jones, E. W. (1991) Tackling the protease problem in *Saccharomyces cerevisiae*. *Methods Enzymol.* **194,** 428–453
86. Sikorski, R. S., and Hieter, P. (1989) A system of shuttle vectors and yeast host strains designed for efficient manipulation of DNA in *Saccharomyces cerevisiae*. *Genetics* **122,** 19–27
87. Veatch, J. R., McMurray, M. A., Nelson, Z. W., and Gottschling, D. E. (2009) Mitochondrial dysfunction leads to nuclear genome instability via an iron-sulfur cluster defect. *Cell* **137,** 1247–1258
88. Harper, J. W., Adami, G. R., Wei, N., Keyomarsi, K., and Elledge, S. J. (1993) The p21 Cdk-interacting protein Cip1 is a potent inhibitor of G_1 cyclin-dependent kinases. *Cell* **75,** 805–816
89. Bartel, P., Chien, C. T., Sternglanz, R., and Fields, S. (1993) Elimination of false positives that arise in using the two-hybrid system. *BioTechniques* **14,** 920–924
90. Jiang, B., and Cyert, M. S. (1999) Identification of a novel region critical for calcineurin function *in vivo* and *in vitro*. *J. Biol. Chem.* **274,** 18543–18551

Table 1. Strains used in this study

Strain	Genotype	Source
BY4743	*MAT***a**/α *his3Δ1/his3Δ1 leu2Δ0/leu2Δ0 LYS2/lys2Δ0 MET15/met15Δ0 ura3Δ0/ura3Δ0*	Open Biosystems (84)
aly1ΔΔ aly2ΔΔ	*MAT***a**/α *his3Δ1/his3Δ1 leu2Δ0/leu2Δ0 LYS2/lys2Δ0 MET15/met15Δ0 ura3Δ0/ura3Δ0 aly1Δ::KanMX4/ aly1Δ::KanMX4 aly2Δ::KanMX4/ aly2Δ::KanMX4*	(24)
BY4741	*MAT***a** *his3Δ1 leu2Δ0 met15Δ0 ura3Δ0*	Open Biosystems (84)
2029	*MAT***a** *his3Δ1 leu2Δ0 met15Δ0 ura3Δ0 npr1Δ::KanMX4*	Open Biosystems (84)
5026	*MAT***a** *his3Δ1 leu2Δ0 met15Δ0 ura3Δ0 lst4Δ::KanMX4*	Open Biosystems (84)
D2-6A	*MAT***a** *his3Δ1 leu2Δ0 MET15 lys2Δ0 ura3Δ0 aly1Δ::KanMX4 aly2Δ::KanMX4*	(24)
4985	*MAT***a** *his3Δ1 leu2Δ0 met15Δ0 ura3Δ0 apl2Δ::KanMX4*	Open Biosystems (84)
BJ5459	*MAT***a** *ura3-52 trp1 lys2-801 leu2Δ1 his3Δ200 pep4Δ::HIS3 prb1Δ1.6R can1 GAL*	(85)
BJ5459-*cnb1Δ::KanMX4*	*MAT***a** *ura3-52 trp1 lys2-801 leu2Δ1 his3Δ200 pep4Δ::HIS3 prb1Δ1.6R can1 GAL cnb1Δ::KanMX4*	This study
BJ5459-*cna1Δ::KanMX4 cna2Δ::NatMX4*	*MAT***a** *ura3-52 trp1 lys2-801 leu2Δ1 his3Δ200 pep4Δ::HIS3 prb1Δ1.6R can1 GAL cna1Δ::KanMX4 cna2Δ::NatMX4*	This study
JR11	*MAT***a** *ura3-52 trp1 lys2-801 leu2Δ1 his3Δ200 pep4Δ::HIS3 prb1Δ1.6R can1 GAL CNA1-GFP::LEU2 CNA2-S-TEV-ZZ::KanMX6*	J. Roy and M.Cyert, unpublished
MKY1800	*MAT*α *his3-200 leu2-3,112 ura3-52 lys2-801 aly1Δ::NatMX4 aly2Δ::NatMX4* DIP5-eGFP::HIS3	I. Möller-Hansen and M. Kaksonen, unpublished
MKY1943	*MAT*α *his3-200 leu2-3,112 ura3-52 lys2-801 aly1Δ::NatMX4* DIP5-eGFP::HIS3	I. Möller-Hansen and M. Kaksonen, unpublished

Strain	Genotype	Source
MKY1791	*MATα his3-200 leu2-3,112 ura3-52 lys2-801* DIP5-eGFP::HIS3	I. Möller-Hansen and M. Kaksonen, unpublished
aly2Δ Dip5-GFP	*MATα his3-200 leu2-3,112 ura3-52 lys2-801 aly2Δ::URA3* DIP5-eGFP::HIS3 (isogenic to MKY1943)	This study
BY4741-EstraD	*MAT***a** *his3Δ1 met15Δ0 ura3Δ0 leu2Δ0::ACT1prom-Estradiol receptor-GAL4::NatMX*	pACT1-GEV was digested with *Eco*RV, transformed into BY4741, and NAT resistant colonies selected. This integrates a gene expressing the estradiol receptor fused to *GAL4* under control of the ACT1 promoter at the *leu2Δ0* locus. (This study)
PJ69-4a	*MAT***a** *his3-200 leu2-3,112 ura3-52 trp1-901 gal4Δ gal80Δ LYS2::GAL1prom-HIS3 GAL2prom-ADE2 met2::GAL7prom-lacZ*	(47)

Table 2. Plasmids used in this study

Plasmid	Genotype	Description (Reference)
pKK212	*CUP1prom* -GST, 2μ, *TRP1*	made by K. Kafadar, unpublished; described in (24)
pKK212-Aly1	*CUP1prom* -GST-*ALY1*, 2μ, *TRP1*	(24)
pKK212-Aly1^{Y686G}	*CUP1prom* -GST-*ALY1*^{Y686G}, 2μ, *TRP1*	Generated using pKK212-Aly1 as a template for site directed mutagenesis with primers mutating Y686 to glycine. (This study)
pKK212-Aly2	*CUP1prom*-GST-*ALY2*, 2μ, *TRP1*	(24)
pKK212-Aly2Y^{703G}	*CUP1prom*-GST-*ALY2Y*^{703G}, 2μ, *TRP1*	Generated using pKK212-Aly2 as a template for site directed mutagenesis with primers mutating Y703 to glycine. (This study)
pKK212-Aly1$^{\Delta PILKIN}$	*CUP1prom* -GST-*ALY1*$^{\Delta PILKIN}$, 2μ, *TRP1*	Generated using pKK212-Aly1 as a template for site directed mutagenesis with primers lacking the PILKIN sequence. (This study)
pKK212-Aly1$^{\Delta PILKIN,Y686G}$	*CUP1prom* -GST-*ALY1*$^{\Delta PILKIN,Y686G}$, 2μ, *TRP1*	Generated using pKK212-Aly1$^{\Delta PILKIN}$ as a template for site directed mutagenesis with primers mutating Y686 to glycine. (This study)
pKK212-Aly1^{PVIVIT}	*CUP1prom* -GST-*ALY1*^{PVIVIT}, 2μ, *TRP1*	Generated using pKK212-Aly1 as a template for site directed mutagenesis with primers that mutate the PILKIN sequence to PVIVIT. (This study)
pKK212-Aly1^{AAAAAA}	*CUP1prom* -GST-*ALY1*^{AAAAAA}, 2μ, *TRP1*	Generated using pKK212-Aly1 as a template for site directed mutagenesis with primers that mutate the PILKIN sequence to AAAAAA. (This study)
pKK212-Aly1^{5A}	*CUP1prom* -GST-*ALY1*^{5A}, 2μ, *TRP1*	Generated using pKK212-Aly1 as a template for site directed mutagenesis with primers that mutate amino acids T250 and S252 to alanines, and then in a second round of mutagenesis with primers that mutate S568, S569, and S573 to alanines. (This study)
pKK212-Aly1^{5E}	*CUP1prom* -GST-*ALY1*^{5E}, 2μ, *TRP1*	Generated using pKK212-Aly1 as a template for site directed mutagenesis with primers that mutate amino acids T250 and S252 to glutamic acids, and then in a second round of mutagenesis with primers that mutate S568, S569, and S573 to glutamic acids. (This study)

Plasmid	Genotype	Description (Reference)
pRS425	2μ, *LEU2*	(86)
pRS425-Aly1	*ALY1prom-ALY1* 2μ, *LEU2*	(24)
pRS425-Aly2	*ALY2prom -ALY2,* 2μ, *LEU2*	(24)
pRS425-Aly1$^{\Delta PILKIN}$	*ALY1prom-ALY1*$^{\Delta PILKIN}$ 2μ, *LEU2*	Generated using pRS425-Aly1 as a template for site directed mutagenesis with primers lacking the PILKIN sequence. (This study)
pRS426	2μ, *URA3*	(86)
pRS426-Aly1	*ALY1prom-ALY1,* 2μ, *URA3*	(24)
pRS426-Aly1^{Y686G}	*ALY1prom-ALY1*^{Y686G}, 2μ, *URA3*	Generated using pRS426-Aly1 as a template for site directed mutagenesis with primers that mutate Y686 to glycine. (This study)
pRS426-Aly2	*ALY2prom-ALY2,* 2μ, *URA3*	(24)
pRS426-Aly2^{Y703G}	*ALY2prom-ALY2*^{Y703G}, 2μ, *URA3*	Generated using pRS426-Aly2 as a template for site directed mutagenesis with primers that mutate Y703 to glycine. (This study)
pRS426-Aly1$^{\Delta PILKIN}$	*ALY1prom-ALY1*$^{\Delta PILKIN}$, 2μ, *URA3*	Subcloned a ~3300 bp *Spe*I/*Xho*I fragment containing Aly1$^{\Delta PILKIN}$ from pRS425-Aly1$^{\Delta PILKIN}$ into pRS426 cut with *Spe*I and *Xho*I restriction enzymes. (This study)
pRS426-Aly1$^{\Delta PILKIN, Y686G}$	*ALY1prom-ALY1*$^{\Delta PILKIN, Y686G}$, 2μ, *URA3*	Generated using pRS426-Aly1$^{\Delta PILKIN}$ as a template for site directed mutagenesis with primers that mutate Y686 to glycine. (This study)
pRS426- Aly1^{5A}	*ALY2prom-ALY1*^{5A}, 2μ, *URA3*	Generated using pRS426-Aly1 as a template for site directed mutagenesis with primers that mutate amino acids T250 and S252 to alanines, and then in a second round of mutagenesis with primers that mutate S568, S569, and S573 to alanines. (This study)
pRS426- Aly1^{5E}	*ALY2prom-ALY1*^{5E}, 2μ, *URA3*	Generated using pRS426-Aly1 as a template for site directed mutagenesis with primers that mutate amino acids T250 and S252 to glutamic acids, and then in a second round of mutagenesis with primers that mutate S568, S569, and S573 to glutamic acids. (This study)
pRS315	2μ, *LEU2*	(86)

Plasmid	Genotype	Description (Reference)
pRS315-Aly1	*ALY1prom-ALY1*, 2μ, *LEU2*	Subcloned a ~3300 bp *Spe*I/*Xho*I fragment containing Aly1 from pRS425-Aly1 into pRS315 cut with *Spe*I and *Xho*I restriction enzymes. (This study)
pRS315-Aly2	*ALY2prom-ALY2*, 2μ, *LEU2*	Subcloned a ~4100 bp *Spe*I/*Xho*I fragment containing Aly2 from pRS425-Aly2 into pRS315 cut with *Spe*I and *Xho*I restriction enzymes. (This study)
pRS315-Aly1$^{\Delta PILKIN}$	*ALY1prom-ALY1*$^{\Delta PILKIN}$, 2μ, *LEU2*	Subcloned a ~3300 bp *Spe*I/*Xho*I fragment containing Aly1$^{\Delta PILKIN}$ from pRS425-Aly1$^{\Delta PILKIN}$ into pRS315 cut with *Spe*I and *Xho*I restriction enzymes. (This study)
pRS315- Aly1^{5A}	*ALY2prom-ALY1*^{5A}, 2μ, *LEU2*	Subcloned a ~3300 bp *Spe*I/*Xho*I fragment containing Aly1^{5A} from pRS425-Aly1^{5A} into pRS315 cut with *Spe*I and *Xho*I restriction enzymes. (This study)
pRS315- Aly1^{5E}	*ALY2prom-ALY1*^{5E}, 2μ, *LEU2*	Subcloned a ~3300 bp *Spe*I/*Xho*I fragment containing Aly1^{5E} from pRS425-Aly1^{5E} into pRS315 cut with *Spe*I and *Xho*I restriction enzymes. (This study)
pCK230	*GAP1prom-GAP1*-sGFP, CEN, *URA3*	(22)
pACT1-GEV	*ACT1prom-Estradiol receptor-GAL4* in pRS40NAT	(87)
pACT2	*ADH1prom-GAL4*-TAD, 2μ, *LEU2*	(88)
Aly1-TAD (1-915)	*ADH1prom-GAL4*-TAD-*ALY1*, 2μ, *LEU2*	*ALY1* coding sequence was PCR amplified from pKK212-*ALY1* with primers containing *Xma*I and *Xho*I restriction site adaptors. The PCR product was then subcloned into pACT2. (This study)
Aly1-TAD (1-609)	*ADH1prom-GAL4*-TAD-*ALY1(1-609)*, 2μ, *LEU2*	*ALY1* sequence encoding amino acids 1-609 was PCR amplified from pKK212-*ALY1* with primers containing *Xma*I and *Xho*I restriction site adaptors. The PCR product was then subcloned into pACT2. (This study)

Plasmid	Genotype	Description (Reference)
Aly1-TAD (610-915)	*ADH1prom-GAL4*-TAD-*ALY1(610-915)*, 2μ, *LEU2*	*ALY1* sequence encoding amino acids 610-915 was PCR amplified from pKK212-*ALY1* with primers containing *Xma*I and *Xho*I restriction site adaptors. The PCR product was then subcloned into pACT2. (This study)
Aly1-TAD (493-915)	*ADH1prom-GAL4*-TAD-*ALY1(493-915)*, 2μ, *LEU2*	*ALY1* sequence encoding amino acids 493-915 was PCR amplified from pKK212-*ALY1* with primers containing *Xma*I and *Xho*I restriction site adaptors. The PCR product was then subcloned into pACT2. (This study)
Aly1-TAD (725-915)	*ADH1prom-GAL4*-TAD-*ALY1(725-915)*, 2μ, *LEU2*	*ALY1* sequence encoding amino acids 725-915 was PCR amplified from pKK212-*ALY1* with primers containing *Xma*I and *Xho*I restriction site adaptors. The PCR product was then subcloned into pACT2. (This study)
Aly1-TAD (610-751)	*ADH1prom-GAL4*-TAD-*ALY1(610-751)*, 2μ, *LEU2*	*ALY1* sequence encoding amino acids 610-751 was PCR amplified from pKK212-*ALY1* with primers containing *Xma*I and *Xho*I restriction site adaptors. The PCR product was then subcloned into pACT2. (This study)
Aly1-TAD (610-831)	*ADH1prom-GAL4*-TAD-*ALY1(610-831)*, 2μ, *LEU2*	*ALY1* sequence encoding amino acids 610-831 was PCR amplified from pKK212-*ALY1* with primers containing *Xma*I and *Xho*I restriction site adaptors. The PCR product was then subcloned into pACT2. (This study)
Aly1-TAD (838-915)	*ADH1prom-GAL4*-TAD-*ALY1(838-915)*, 2μ, *LEU2*	*ALY1* sequence encoding amino acids 838-915 was PCR amplified from pKK212-*ALY1* with primers containing *Xma*I and *Xho*I restriction site adaptors. The PCR product was then subcloned into pACT2. (This study)
Aly1-TAD (822-915)	*ADH1prom-GAL4*-TAD-*ALY1(822-915)*, 2μ, *LEU2*	*ALY1* sequence encoding amino acids 822-915 was PCR amplified from pKK212-*ALY1* with primers containing *Xma*I and *Xho*I restriction site adaptors. The PCR product was then subcloned into pACT2. (This study)
Aly1$^{\Delta PILKIN}$-TAD	*ADH1prom-GAL4*-TAD-*ALY1*$^{\Delta PILKIN}$, 2μ, *LEU2*	*ALY1*$^{\Delta PILKIN}$ sequence was PCR amplified from pKK212- ALY1$^{\Delta PILKIN}$ with primers containing *Xma*I and *Xho*I restriction site adaptors. The PCR product was then subcloned into pACT2. (This study)

Plasmid	Genotype	Description (Reference)
Aly2-TAD	*ADH1prom-GAL4*-TAD-*ALY2*, 2μ, *LEU2*	*ALY2* coding sequence was PCR amplified from pKK212-*ALY2* with primers containing *Xma*I and *Xho*I restriction site adaptors. The PCR product was then subcloned into pACT2. (This study)
Rod1-TAD	*ADH1prom-GAL4*-TAD-*ROD1*, 2μ, *LEU2*	*ROD1* coding sequence was PCR amplified from genomic DNA with primers containing *Xma*I and *Sac*I restriction site adaptors. The PCR product was then subcloned into pACT2. (This study)
Rog3-TAD	*ADH1prom-GAL4*-TAD-*ROG3*, 2μ, *LEU2*	*ROG3* coding sequence was PCR amplified from genomic DNA with primers containing *Xma*I and *Xho*I restriction site adaptors. The PCR product was then subcloned into pACT2. (This study)
Ldb19-TAD	*ADH1prom-GAL4*-TAD-*LDB19*, 2μ, *LEU2*	*LDB19* coding sequence was PCR amplified from genomic DNA with primers containing *Xma*I and *Xho*I restriction site adaptors. The PCR product was then subcloned into pACT2. (This study)
Ecm21-TAD	*ADH1prom-GAL4*-TAD-*ECM21*, 2μ, *LEU2*	*ECM21* coding sequence was PCR amplified from genomic DNA with primers containing *Xma*I and *Xho*I restriction site adaptors. The PCR product was then subcloned into pACT2. (This study)
Csr2-TAD	*ADH1prom-GAL4*-TAD-*CSR2*, 2μ, *LEU2*	*CSR2* coding sequence was PCR amplified from genomic DNA with primers containing *Xma*I and *Xho*I restriction site adaptors. The PCR product was then subcloned into pACT2. (This study)
Art10-TAD	*ADH1prom-GAL4*-TAD-*ART10*, 2μ, *LEU2*	*ART10* coding sequence was PCR amplified from genomic DNA with primers containing *Xma*I and *Xho*I restriction site adaptors. The PCR product was then subcloned into pACT2. (This study)
Art5-TAD	*ADH1prom-GAL4*-TAD-*ART5*, 2μ, *LEU2*	*ART5* coding sequence was PCR amplified from genomic DNA with primers containing *Xma*I and *Xho*I restriction site adaptors. The PCR product was then subcloned into pACT2. (This study)

Plasmid	Genotype	Description (Reference)
Bul1-TAD	*ADH1prom-GAL4*-TAD-*BUL1*, 2μ, *LEU2*	*BUL1* coding sequence was PCR amplified from genomic DNA with primers containing *Xma*I and *Sac*I restriction site adaptors. The PCR product was then subcloned into pACT2. (This study)
Bul2-TAD	*ADH1prom-GAL4*-TAD-*BUL2*, 2μ, *LEU2*	*BUL2* coding sequence was PCR amplified from genomic DNA with primers containing *Xma*I and *Xho*I restriction site adaptors. The PCR product was then subcloned into pACT2. (This study)
CNB-TAD (human)	*ADH1prom-GAL4*-TAD-*CNB*, 2μ, *LEU2*	The calcineurin regulatory subunit (CNB) from *Homo sapiens* was PCR amplified from a clone obtained from Open Biosystems with primers containing *Bam*HI and *Xho*I restriction site adaptors. The PCR product was cloned into pACT2. (This study)
pGBT9	*ADH1prom-GAL4*-DBD, 2μ, *TRP1*	(89)
DBD-Cna1 (yeast)	*ADH1prom-GAL4*-DBD-*CNA1*, 2μ, *TRP1*	(90)
DBD-CNA (human)	*ADH1prom-GAL4*-DBD-*CNA* isoform α, 2μ, *TRP1*	The calcineurin catalytic subunit (CNA) isoform α from *Homo sapiens* was PCR amplified from a clone obtained from Open Biosystems with primers containing *Bam*HI restriction site adaptors. The PCR product was cloned into pGBT9. (This study)